APPENDIX C
HAZARD ANALYSIS

WORST-CASE CONSEQUENCE ANALYSIS
FOR ULTRAMAR'S WILMINGTON REFINERY
ALKYLATION IMPROVEMENT PROJECT

Prepared For

Environmental Audit, Inc.
1000-A Ortega Way
Placentia, California 92670-7125

Prepared By

Quest Consultants Inc.
908 26th Avenue N.W.
Norman, Oklahoma 73069
Telephone: 405-329-7475
Fax: 405-329-7734

04-01-6481
January 12, 2004

QUEST

WORST-CASE CONSEQUENCE ANALYSIS FOR ULTRAMAR'S WILMINGTON REFINERY ALKYLATION IMPROVEMENT PROJECT

Table of Contents

QUEST

Table of Contents
(Continued)

QUEST

List of Tables

List of Figures

QUEST

SECTION 1
INTRODUCTION

Quest Consultants Inc. was retained by Ultramar to perform a worst-case consequence analysis on the process unit modifications and additions to Ultramar's Wilmington Refinery. The proposed process modifications and additions are related to Ultramar's decision to increase aklylate production and eliminate the use of pure hydrofluoric acid in the alkylation unit by licensing Phillips' ReVAP process. The objective of the study was to compute the potential decrease and/or increase in hazard to the public due to the proposed process unit modifications and additions.

The study was divided into three tasks.

Task 1. Determine the maximum credible potential releases, and their consequences, for existing process units and storage areas.

Task 2. Determine the maximum credible potential releases and their consequences for new units to be added or those which have been proposed for modification by Ultramar.

Task 3. Determine whether the consequences associated with the proposed modifications or additions generate a potential hazard that is larger than the potential hazard which currently exists at the facility.

Potential hazards from the existing, modified, and new equipment are associated with accidental releases of toxic/flammable gas, toxic/flammable liquefied gas, and flammable and combustible liquids. Hazardous events associated with gas releases include toxic gas clouds, torch fires, and vapor cloud explosions. Hazardous events associated with potential releases of toxic/flammable liquefied gases include toxic clouds, torch fires, flash fires, and vapor cloud explosions. Releases of flammable or combustible liquids may result in pool fires.

One hazard of interest for a release of toxic/flammable gas or liquefied gas is exposure to a gas cloud. For such releases, this study evaluates the extent of possible exposure to gas clouds containing hydrofluoric acid (HF) or hydrogen sulfide (H_2S).

The hazard of interest for flash fires is direct exposure to the flames. Flash fire hazard zones are determined by calculating the maximum size of the flammable gas cloud prior to ignition. These hazard zones are defined by the lower flammable limit (LFL) of the released hydrocarbon mixture. For vapor cloud explosions, the hazard of interest is the overpressure created by the blast wave. The hazard of interest for torch fires and pool fires is fire radiation. For Boiling Liquid–Expanding Vapor Explosions (BLEVEs), the hazard of interest is the radiation produced by the fireball.

For each type of hazard identified (toxic, radiant, overpressure), maximum distances to potentially injurious levels are determined. The hazard levels have been approved by the Southern California Air Quality Management District (SCAQMD).

QUEST

SECTION 2
OVERVIEW OF ULTRAMAR'S WILMINGTON REFINERY

2.1   Facility Location

Ultramar's Wilmington Refinery is located in the southern portion of Los Angeles County at 2402 East Ana-
heim Street, Wilmington, California. The refinery is bounded by Anaheim Street to the north, Dominguez
Channel to the west, and industrial areas to the south and east. The Terminal Island Freeway passes through
the middle of the facility. Layout of the refinery and major roads bounding the facility are presented in Figure
2-1.

The process units, storage facilities, and product transfer systems included in the project are listed in Table
2-1. Table 2-1 identifies which of the existing units involved in the project will be modified as part of the
project. Unit locations within Ultramar are shown in Figure 2-1.

2.2   Meteorological Data

Meteorological data for the Los Angeles area were reviewed to determine representative values for tempera-
ture and relative humidity. Wind speed and stability class were also reviewed to determine the range of con-
ditions that are possible at the site. In this study, a low wind/stable condition (1.5 m/s wind, "F" stability)
was evaluated for each dispersion calculation. These conditions often approximate the worst-case weather
conditions for dispersion analysis. For the purposes of this analysis, the vapor cloud was assumed to travel
in any direction with equal probability. When performing pool fire and torch fire calculations, a high wind
that "bends" the flame is considered a worst-case condition. In this study, all fire radiation calculations were
performed using 6 m/s winds.

2.3   Description of Units Involved in the Wilmington Refinery Alkylation Improvement Project

2.3.1   Modified Process Units

2.3.1.1 Modifications to Existing Alkylation Unit

In order to incorporate ReVAP into the existing Alkylation Unit and to enhance the alkylate production
capacity to 20,000 bpd, modifications are required to the individual sections of the unit, as discussed below.
Alkylate production will continue to follow the basic process flow, with changes to the following process and
equipment.

- Modifications to the HF Acid Storage, Replenishment, and Injection Section
  The existing Acid Storage Drum will be used to store the modified HF. A new recycle additive
  surge tank will provide sufficient surge volume for rapid additive concentration control in the
  reactor system acid. This vessel will also serve as a unit additive storage vessel at times when the
  unit is shut down for maintenance.

- Modifications to the Reaction and Settling Section
  The ReVAP process requires larger reactors and a higher circulation rate than the present process.
  Two new alkylation reactors will be installed to operate in combination with the two existing

QUEST
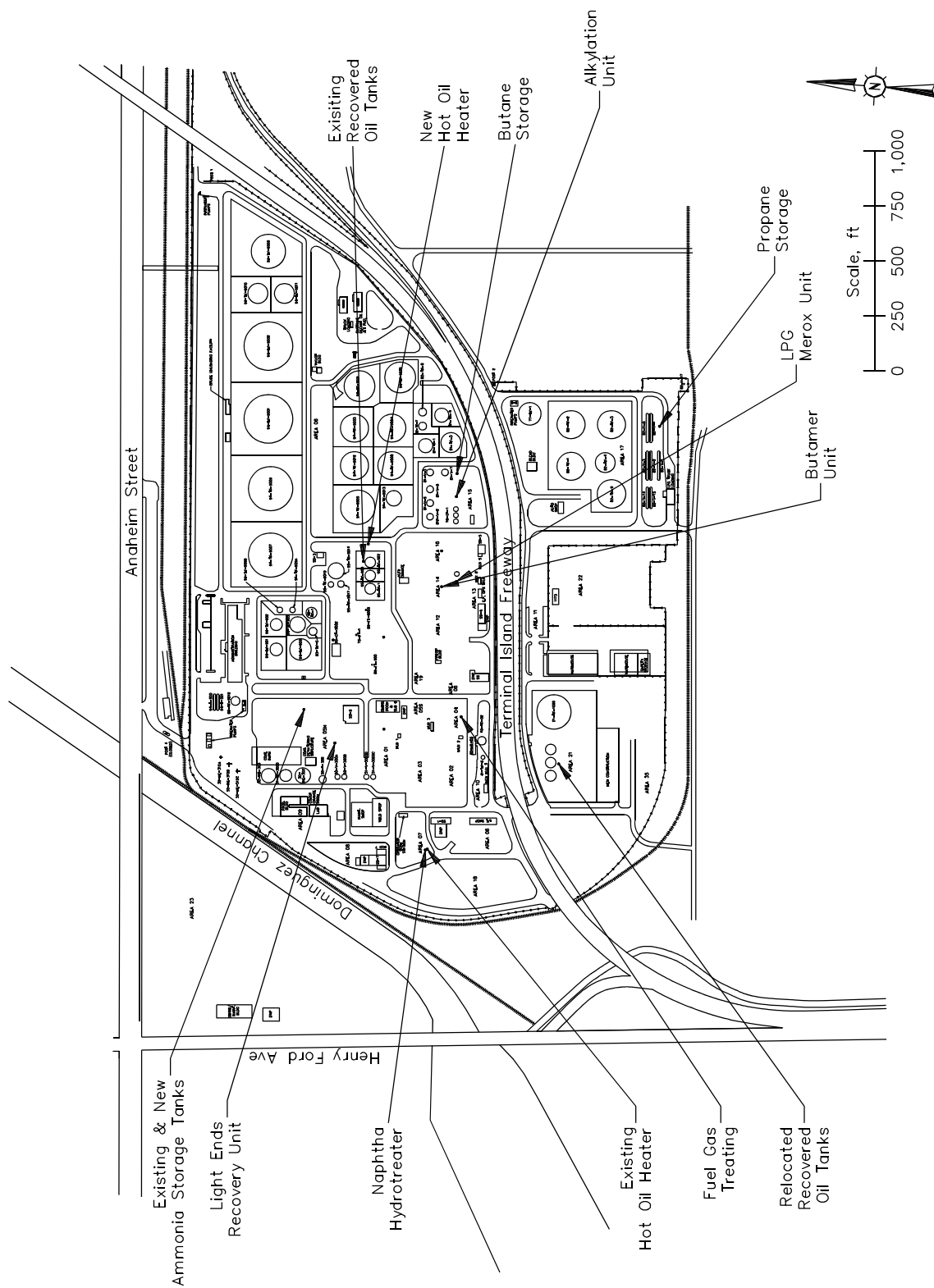
Figure 2-1
Location of Process Units to be Modified or Added within the Ultramar Refinery

QUEST

Table 2-1
Process Units and Facilities Involved in the Refinery Alkylation Improvement Project

Designation	Description	Existing/New	To Be Modified
Process Units			
ALKY	Alkylation Unit	Existing	Yes
FGTU	Fuel Gas Treating Unit	New	---
NHT	Naphtha Hydrotreating Unit	Existing	Yes
BUTAMER	Butamer Unit	Existing	Yes
LER1	Light Ends Recovery Unit	Existing	Yes
LER2	Light Ends Recovery Unit	Existing	Yes
MEROX	LPG Merox Unit	Existing	Yes
Storage			
TANK	Atmospheric Storage	Existing	Yes
AQNH3 TANK	Aqueous Ammonia Storage Tank	New	---
LPG	Pressurized Storage	Existing	No
	Pressurized Storage	New	---
Auxiliary Facilities			
HOH	Hot Oil Heater for Isobutanizer Tower and Deisobutanizer	New	---
BOILER	Steam Boiler	New	---

alkylation reactors. The existing two acid circulation pumps will be replaced with two new larger capacity pumps.

- Modified Product Separation (Fractionation) Section
  A Recontactor will be added to reduce the fluoride content of the feed to the Fractionation Section and to remove excessive acid from the feed to the fractionators. After separation of acid and hydrocarbon phases in the Recontactor, the hydrocarbon phase enters the Fractionation Section and excess is pumped back to the reactor acid pump section. The narrower top section of the Depropanizer will be replaced with one having a larger diameter to handle incrementally larger amounts of propane in the Alkylation Unit feed.

- Modified HF Stripping Section
  The existing butane alumina treaters and propane alumina treaters will be replaced with new treaters, and a new propane potassium hydroxide (KOH) treater will be installed and operate with the existing propane KOH treater to meet the enhanced Alkylation Unit operation requirements.

- New Additive Recovery from the Alkylate Product
  Trace amounts of ReVAP additive in the Isostripper alkylate product will be removed by a water wash extraction process in a new water wash column. The dilute additive/water stream from the water wash column bottoms is fed to the new evaporator column, which is mounted on the evaporator column kettle reboiler. The evaporator column concentrates the additive in the bottoms product.

QUEST

- Modified HF Regeneration Section
  The existing acid regeneration system is undersized for the acid soluble oil (ASO) that will be produced at the new alkylate production rates and will be replaced. A new rerun column will produce both a side draw stream for water removal and a bottoms product for ASO removal.

2.3.1.2 Modifications to the Existing Butamer Unit

In order to provide sufficient isobutane for enhanced alkylate, the refinery proposes to upgrade the capacity of the Butamer Unit from 10,000 bpd to 17,000 bpd. To accomplish this will require a combination of new components and increasing the size (referred to as "debottlenecking") of the Deisobutanizer (DIB) column and related equipment.

The principal changes will be in the DIB (fractionation) column. The DIB column is both a tall and a large diameter column. Fractionation of isobutane from normal butane requires a relatively large number of fractionation stages due to the narrow boiling point difference between the light and heavy components. In its current configuration, the DIB has two reboilers, one heated with process waste heat and the second heated with steam. For the enhancement project, a new steam reboiler operating in parallel with the existing boiler is proposed as a replacement for the waste heat reboiler, which will be used as a feed preheater. Other changes are proposed to improve the energy efficiency (steam requirements) of the unit.

2.3.1.3 Modifications to the Existing LPG Merox Treating Unit

Mercaptan, sulfur, and traces of hydrogen sulfide from butanes, which could poison the Butamer Unit catalyst and affect the alkylate product, are removed in LPG Merox Unit by caustic wash. The LPG Merox Unit capacity must be increased from 6,500 bpd of field butanes to treat 10,000 bpd. The only modification required is replacement of existing caustic prewash drum with a new larger vessel.

2.3.1.4 Modifications to the Existing Light Ends Recovery Unit

The light ends recovery unit processes naphtha and byproduct gases from various units. Minor modifications to this unit will allow more butane to be desulfurized in the Naphtha Hydrotreater (NHT) for feed to the Butamer Unit. Principal modifications include a new depropanizer feed drum and feed pumps, replacement of depropanizer tower trays, vessel and reboiler tube replacement, and new heat exchangers.

2.3.1.5 Modifications to the Existing Naphtha Hydrotreater Unit

The Naphtha Hydrotreater removes organic sulfur, oxygen, nitrogen, metals, and other compounds from hydrocarbon fractions. Minor modifications will be made to provide sufficient LPG feed for the modified alkylation process. Principal modifications include a new debutanizer complex and modifications to heat exchangers and pumps. The new debutanizer separates the butane and light straight runs. The butane will be routed to the Light End Recovery Unit for recovery of butane for the Butamer Unit.

QUEST

2.3.2 New Process Units

2.3.2.1 Proposed New Fuel Gas Treating System

The refinery will install a new fuel gas treating system to reduce the sulfur content of the additional fuel gas to be consumed as a result of the Alkylation Unit improvements. The process uses a fiber contactor system to treat fuel gas with a circulating stream of amine and caustic to remove hydrogen sulfide, carbonyl sulfide, and mercaptans.

2.3.3 Utilities and Auxiliary Facilities

The proposed conversion to ReVAP and enhanced operation of the Alkylation Unit will require additional steam.

2.3.3.1 New Steam Boiler

The refinery steam demand is expected to increase by approximately 200,000 pounds per hour (lb/hr) due to the Alkylation Unit modifications. A new 245 million British thermal units per hour (mmBtu/hour) boiler will be installed to produce 300 pounds per square inch steam. The boiler will be equipped with selective catalytic reduction (SCR) control equipment in accordance with SCAQMD requirements.

2.3.3.2 New Hot Oil Heater

A new 350 million Btu/hour Hot Oil Heater system will be installed to provide the heat source required to reboil the Isostripper Tower and the DIB in the Butamer. An SCR will be installed on the new heater for nitrogen oxide (NOx) control.

2.3.4 Storage

2.3.4.1 New Butane Storage Sphere

The increased flow of normal butane feed for the Butamer Unit will require a new 5,000 barrel pressurized Butane Storage Sphere. Butanes from the refinery, as well as purchased butanes, will be stored in the new butane storage sphere. New butane transfer pumps will pump butane from this sphere to the Butamer Unit.

2.3.4.2 New Propane Storage Bullet

The modified Alkylation Unit will increase the production of propane product due to the increase in alkylation capacity. This will require a new 4,000 barrel Pressurized Propane Storage Bullet to store the added production. New propane transfer pumps will pump propane from this propane storage bullet to the existing truck loading facility.

QUEST

2.3.4.3 <u>New Aqueous Ammonia Tank</u>

A new 15,000 gallon storage tank is proposed to store aqueous ammonia associated with the SCR Unit for the new Boiler.

2.3.4.4 <u>Storage Tank Relocation</u>

There are three storage tanks located immediately north of the Alkylation Unit and Butamer Unit, which will be removed to accommodate the improvements to the Alkylation Unit. The tanks will be relocated to Area 21 in the southwest corner of the refinery property, within the vicinity of TK 1000.

QUEST

SECTION 3
POTENTIAL HAZARDS

3.1   Hazards Identification

The potential hazards associated with Ultramar's existing Wilmington Refinery and those associated with the new units and proposed modifications to the existing units identified in Section 2 are common to most refineries worldwide, and are a function of the materials being processed, processing systems, procedures used for operating and maintaining the facility, and hazard detection and mitigation systems. The hazards that are likely to exist are identified by the physical and chemical properties of the materials being handled and the process conditions. For hydrocarbon fuel and petrochemical facilities, the common hazards are:

- toxic gas clouds (gas or liquefied gas with hydrogen fluoride or hydrogen sulfide)
- torch fires (gas and liquefied gas releases)
- flash fires (liquefied gas releases)
- pool fires (flammable/combustible liquid releases)
- vapor cloud explosions (gas and liquefied gas releases)
- BLEVEs (major failures of liquefied gas storage tanks)

The Ultramar facility under evaluation was divided into three types of areas: process, storage, and auxiliary facilities. The hazards expected to be identified in each of the three areas are listed in Table 3-1.

3.2   Introduction to Physiological Effects of Toxic Gases, Fires, and Explosions

The analysis performed on the Ultramar Refinery modifications involved the evaluation of hundreds of potential hazardous material releases. The potential releases may result in one or more of the following hazards:

- Exposure to toxic gas
    Hydrogen fluoride
    Hydrogen sulfide
- Exposure to flame radiation
    Pool fire (tank fire, spill into diked areas)
    Torch fire (rupture of line followed by ignition)
    BLEVE (Boiling Liquid–Expanding Vapor Explosion of a pressurized storage vessel)
    Flash fires (ignition of slow-moving flammable vapors)
- Exposure to explosion overpressure
    Vapor cloud explosion (release, dispersion, and explosion of a flammable vapor cloud)
    Confined explosion (ignition and explosion of flammable vapors within a building or confined area)

In order to compare the hazards associated with each type of hazard listed above, a common measure of consequence or damage must be defined. In consequence and risk analysis studies, a common measure for such hazards is their impact on humans. For each of the toxic, fire, and explosion hazards listed, there are data available that define the effect of the hazard on humans.

When comparing a toxic hazard to a flammable or explosive hazard, the magnitude of the hazard's impact on humans must be identically defined. For instance, it would not be meaningful to compare human exposure

QUEST

Table 3-1
Summary of Hazards

Area Description	Type of Hazards Found in Area

Process areas
    NHT
    LER1
    LER2
    MEROX
    ALKY
    FGTU
    BUTAMER
	Breach of liquid line or vessel resulting in:
	    Pool fire
	Breach of flashing liquid line or vessel resulting in:
	    Flash fire
	    Vapor cloud explosion
	    Pool fire
	    Torch fire
	    Toxic cloud (hydrogen fluoride, hydrogen sulfide)
	Breach of vapor line or vessel resulting in:
	    Torch fire
	    Vapor cloud explosion
	    Toxic cloud (hydrogen fluoride, hydrogen sulfide)

Storage
    TANK
    LPG
    AQNH3 TANK
	Breach of atmospheric storage resulting in:
	    Tank fire
	    Impounding area fire
	    Toxic cloud (ammonia)
	Breach of flashing liquid line or vessel resulting in:
	    Flash fire
	    Vapor cloud explosion
	    Pool fire
	    Torch fire
	BLEVE of pressurized storage vessel

Auxiliary systems
    HOH
    BOILER
	Breach of low pressure piping resulting in:
	    Pool fire
	Breach of vapor line resulting in:
	    Torch fire

to nonlethal overpressures (low overpressures which break windows) to human exposure to lethal fire radiation (34,500 Btu/(hr·ft^2) for five seconds). Thus, in order to compare the hazards of toxic gases, fires, and explosions on humans, equivalent levels of hazard must be defined.

The endpoint hazard criterion defined in this study corresponds to a hazard level which might cause an injury. With this definition, the injury level must be defined for each type of hazard (toxic, radiant heat, or overpressure exposure). The South Coast Air Quality Management District has defined equivalent injury levels for each of the hazards listed. Table 3-2 presents endpoint hazard criteria approved by SCAQMD for this work.

3.3**Selection of Accidental Release Case Studies**

3.3.1**Overview of Methodology**

The purpose of the hazard case selection methodology is to define the maximum credible hazard scenario for each unit that might result in an impact to the public. The methodology is developed in seven increments:

QUEST

Table 3-2
Consequence Analysis Hazard Levels
(Endpoint Criteria for Consequence Analysis)

Hazard Type	Injury Threshold		
	Exposure Duration	Hazard Level	Reference
Hydrogen fluoride	Up to 60 min	20 ppm	ERPG-2 [AIHA, 1988] 40 CFR 68 [EPA, 1996]
Hydrogen sulfide inhalation	Up to 60 min	30 ppm	ERPG-2 [AIHA, 1988] 40 CFR 68 [EPA, 1996]
Radiant heat exposure	40 sec	1,600 Btu/(hr·ft^2)*	40 CFR 68 [EPA, 1996]
Explosion overpressure	Instantaneous	1.0 psig**	40 CFR 68 [EPA, 1996]
Flash fires (fireballs)	40 sec	1,600 Btu/(hr·ft^2)*	40 CFR 68 [EPA, 1996]
Flash fires (flammable vapor clouds)	Instantaneous	LFL	40 CFR 68 [EPA, 1996]

ERPG-2. The maximum airborne concentration below which it is believed nearly all individuals could be exposed for up to one hour without experiencing or developing irreversible or other serious health effects or symptoms that could impair an individual's ability to take protective action.
40 CFR 68. United States Environmental Protection Agency RMP endpoints.
 * Corresponds to second-degree skin burns.
** Corresponds to partial demolition of houses.

- Initial review
- Detailed review of process flow diagrams
- Review of process material balances
- Review of available safety studies
- Development of hazard scenarios
- Screening of hazard scenarios via hazards analysis
- Final selection of hazard cases

3.3.2 Initial Review

The analysis begins with a general review of the process. Any written description of the new or modified processes is studied to determine the physical and chemical transformations occurring and the general flow of material in the unit. After the process features are known, process flow diagrams (PFDs) are reviewed and compared to the written descriptions.

3.3.3 Detailed Review of Process Flow Diagrams

The detailed review of the PFDs begins by tracing the major process flow lines in the unit. When the major flows within the unit are found, the material balances are reviewed for each major line to determine the exact nature of the material within the line or vessel.

QUEST

Each of the major flow lines is taken individually and evaluated to determine the potential for producing a major hazard if a leak or rupture occurred. At this point in the analysis, a list of potential areas of concern is started; this list is continually refined and added to during the remaining analysis steps.

Several factors are involved in the initial selection of hazard areas:

• Flammability and/or toxic nature of the chemicals
• Potential for aerosol formation (releases of streams considerably above their atmospheric boiling point)
• Line size
• Normal flow rate in the line
• Severity of the process conditions

The factors described above are not weighted equally in the evaluation. The flammability and/or toxic nature, potential for aerosol formation, and process conditions are given more weight than the other factors.

3.3.4   Review of Process Material Balances

Although the process material balances have been reviewed for each major process flow line, they are more thoroughly reviewed during this stage of the analysis to locate points in the process where toxic materials and/or materials sensitive to detonation are used.

A spreadsheet describing the material balances for the identified hazard locations is begun. The material balance gives the molar flows, the mass flows, and the mole fraction of the components of each process stream. The stream temperature, pressure, and line size are also noted in the spreadsheet. As additional hazard areas are found, their stream summaries are added to the spreadsheet.

3.3.5   Review of Previous Safety Studies

Previous safety studies, including HAZOP reports, "What if?" analyses, safety audits, etc., are reviewed to determine if all potential hazard areas have been adequately identified. Any potential hazards identified in these work products are added to the list of potential areas of concern that was started during the detailed review of the PFDs.

3.3.6   Development of Hazard Scenarios

The list of potential hazard areas developed in the preceding analysis stages is put into a spreadsheet. The spreadsheet contains the following information:

• Case number
• Description of the area where release originates (line, vessel, etc.)
• Stream number found on the PFDs
• Stream or vessel temperature
• Stream or vessel pressure
• Assessment of the physical state of the stream (gas, liquid, two-phase)
• Total volume of the vessel or the nearest vessel
• Liquid volume of the vessel or the nearest vessel

QUEST

- Line size
- Normal flow rate of the line or vessel

3.3.7   Initial Screening via Hazard Zone Analysis

The hazard zones resulting from the worst-case releases of similar hazard scenarios are evaluated to determine the process areas that could release material with a potential for public impact. When performing site-specific consequence analysis studies, the ability to accurately model the release, dilution, and dispersion of gases and aerosols is important if an accurate assessment of potential exposure is to be attained. For this reason, Quest uses a modeling package, CANARY by Quest®, that contains a set of complex models that calculate release conditions, initial dilution of the vapor (dependent upon the release characteristics), and the subsequent dispersion of the vapor introduced into the atmosphere. The models contain algorithms that account for thermodynamics, mixture behavior, transient release rates, gas cloud density relative to air, initial velocity of the released gas, and heat transfer effects from the surrounding atmosphere and the substrate. The release and dispersion models contained in the QuestFOCUS package (the predecessor to CANARY by Quest) were reviewed in a United States Environmental Protection Agency (EPA) sponsored study [TRC, 1991] and an American Petroleum Institute (API) study [Hanna, Strimaitis, and Chang, 1991]. In both studies, the QuestFOCUS software was evaluated on technical merit (appropriateness of models for specific applications) and on model predictions for specific releases. One conclusion drawn by both studies was that the dispersion software tended to overpredict the extent of the gas cloud travel, thus resulting in too large a cloud when compared to the test data (i.e., a conservative approach).

A study prepared for the Minerals Management Service [Chang, et al.,1998] reviewed models for use in modeling routine and accidental releases of flammable and toxic gases. CANARY by Quest received the highest possible ranking in the science and credibility areas. In addition, the report recommends CANARY by Quest for use when evaluating toxic and flammable gas releases. The specific models (e.g., SLAB) contained in the CANARY by Quest software package have also been extensively reviewed. Technical descriptions of the CANARY models used in this study are presented in Appendix A.

3.3.8   Final Selection of Hazard Cases

Using the data collected in the hazard area spreadsheet and the initial screening hazard zone calculations, a final selection of hazard cases is made. These selections generally define the maximum extent of any credible potential hazard that could occur in the process area being evaluated.

QUEST

SECTION 4
WORST-CASE CONSEQUENCE MODELING RESULTS

The results of the worst-case consequence modeling calculations for the new, modified, and existing units are presented in this section. In addition, several hazard zones are overlaid onto the facility map in order to demonstrate the possible public exposure to the defined hazard levels.

4.1   Releases Resulting in the Largest Downwind Hazard Zones

With the completion of the hazard identification and consequence modeling calculations described in Section 3 for both the existing and proposed Ultramar configurations, the release from each unit which generates the largest hazard zone can be identified. These releases are listed in Table 4-1. As can be seen from Table 4-1, most of the proposed modifications do not affect the equipment location where the largest potential release originates. That is to say, the potential releases which would result in the largest hazard zones are already in place for many of the units. For example, in the Naphtha Hydrotreating Unit (NHT), a rupture of the liquid line leaving the splitter column overhead accumulator results in the largest potential hazard zone (toxic H_2S cloud). The modifications to the NHT do not result in release scenarios which could create hazard zones larger than those from the splitter column overhead accumulator.

4.2   Description of Potential Hazard Zones

4.2.1   Toxic Vapor Clouds

For a potential accident (e.g., pipe break, hole in a vessel, etc.), one particular set of release conditions/atmospheric conditions will create the largest potential hazard zone. As an example, consider a rupture of the liquid line leaving the debutanizer overhead accumulator reflux line in the Naphtha Hydrotreater Unit (NHT). This release scenario only exists for post-project conditions because it reflects a change in the operating conditions of the unit. In the worst-case release scenario, the material is not ignited, resulting in possible exposure to a cloud containing H_2S downwind of the release. Under the worst-case atmospheric conditions evaluated, the toxic hazard zone (as defined by the ERPG-2 H_2S concentration level, 30 ppm) extends 2,150 ft downwind from the point of release. The hazard "footprint" associated with this event is illustrated in two ways in Figure 4-1. One method presents the hazard zone as a circle which extends 2,150 ft around the point of release from the debutanizer overhead accumulator. This presentation, referred to as a vulnerability zone, is misleading since everyone within the circle cannot be simultaneously exposed to a 30 ppm H_2S level from any single accident. A more realistic illustration of the potential hazard zone around the release point is given by the darkened cloud in Figure 4-1. The cloud area illustrates the H_2S hazard footprint that would be expected IF a rupture of the reflux line were to occur, AND the wind is blowing at a low speed to the southwest, AND the atmosphere is calm, AND the vapor cloud does not ignite following release.

4.2.2   Vapor Cloud Explosions

One of the possible results of a flammable liquid or gas release is the ignition of flammable vapors, which could result in a vapor cloud explosion (VCE). An example of an event tree showing the sequence of events that could lead to a VCE is presented in Figure 4-2. As an example, the 1.0 psig vapor cloud explosion overpressure hazard footprint following a rupture of the liquid reflux line leaving the debutanizer overhead

QUEST

Table 4-1
Potential Accidents Resulting in Maximum Potential Hazard

Process Unit/Area	Status of Potential Hazard (E) Existing, (M) Modified, (N) New	Potential Release (Hazard)
ALKY	E	Rupture of liquid line leaving acid settler (HF toxicity)
	M	Rupture of liquid line leaving reactor #2 (HF toxicity)
BUTAMER	E	Rupture of liquid line leaving debutanizer accumulator (flash fire)
	M	Rupture of liquid line leaving debutanizer accumulator (flash fire)
NHT	E	Rupture of liquid line leaving splitter overhead accumulator (flash fire)
	N	Rupture of liquid reflux line leaving debutanizer overhead accumulator (H_2S toxicity)
FGTU	E	Rupture of fuel gas inlet line (H_2S toxicity)
	M	Rupture of fuel gas inlet line (H_2S toxicity)
LER1	E	Rupture of sour gas line leaving debutanizer accumulator (H_2S toxicity)
	M	Rupture of liquid line leaving debutanizer accumulator (H_2S toxicity)
LER2	E	Rupture of liquid line leaving debutanizer accumulator (H_2S toxicity)
	M	Rupture of liquid line leaving debutanizer accumulator (H_2S toxicity)
MEROX	E	Rupture of liquid line leaving caustic prewash (flash fire)
	N	Rupture of liquid line leaving caustic prewash (flash fire)
TANK	E	Tank 95-TK-1 recovered oil tank fire (fire radiation)
	M	Tank 95-TK-1 recovered oil tank fire (fire radiation)
LPG (C3 STORAGE)	E	BLEVE of 2,000 barrel LPG bullet (fire radiation)
	N	BLEVE of 4,000 barrel LPG bullet (fire radiation)
LPG (C4 STORAGE)	E	BLEVE of 4,760 barrel butane sphere (fire radiation)
	N	BLEVE of 5,000 barrel butane sphere (fire radiation)
HOH	E	Rupture of fuel gas line (flash fire)
	M	Rupture of fuel gas line (flash fire)
BOILER	N	Rupture of fuel gas line (flash fire)
AQNH3 TANK	E	Rupture of liquid line from tank (NH_3 toxicity)
	N	Rupture of liquid line from tank (NH_3 toxicity)

accumulator in the NHT is presented in Figure 4-3. This hazard extends 790 ft from the process area where flammable vapors are confined. For explosions that originate in a process area, the hazard footprint is identical to the vulnerability zone.

QUEST

Rupture of Reflux Line Leaving
the Debutanizer Overhead Accumulator
30 ppm H₂S

Anaheim Street

Dominguez Channel

Terminal Island Freeway

Henry Ford Avenue

Scale, ft

0 250 500 750 1,000
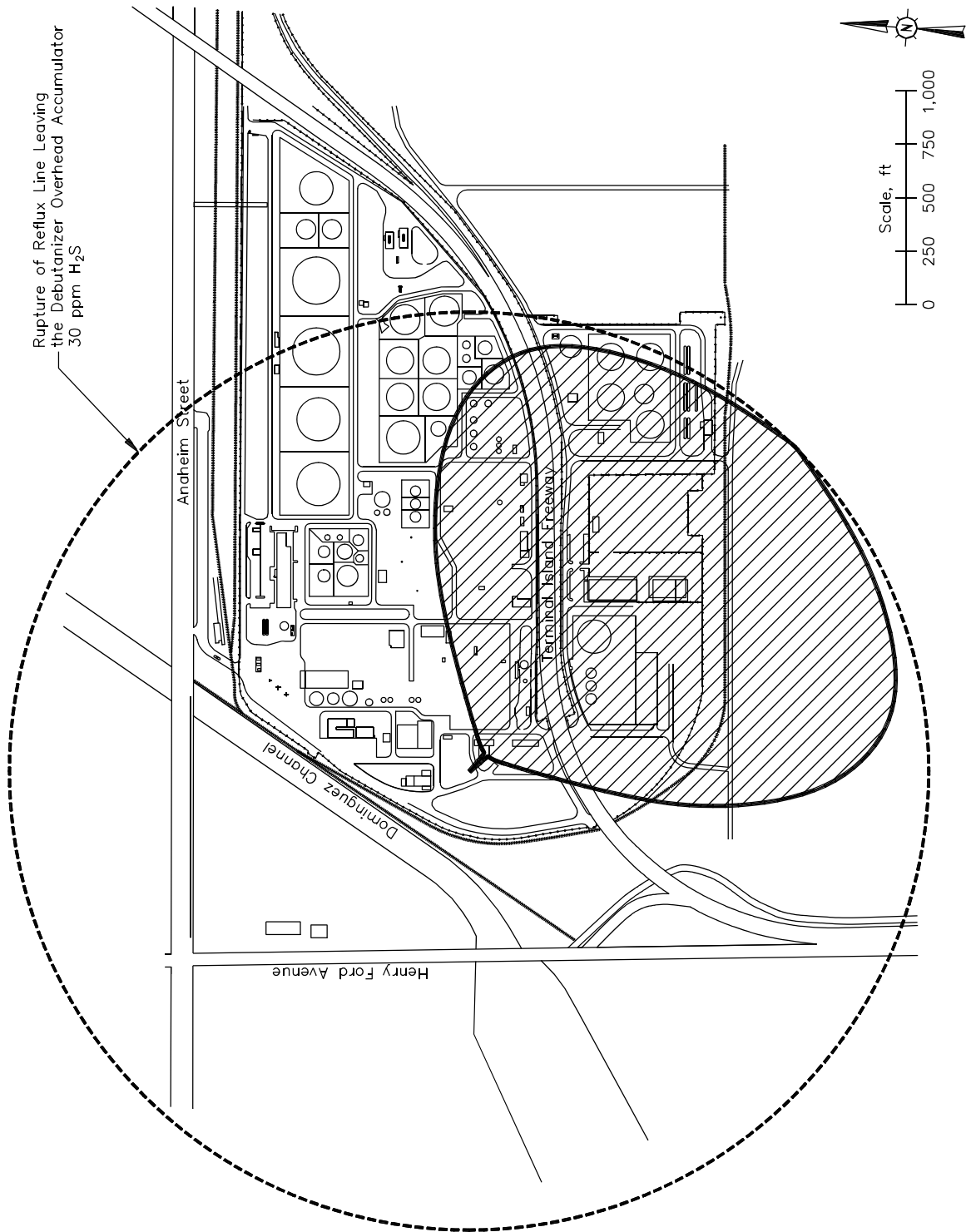
Figure 4-1
Worst-Case Consequence Analysis Hazard Footprint - NHT (H₂S Toxicity)

QUEST

Outcome

Release of Liquid or
Liquefied Gas from
High-Pressure Piping
Pipe Diameter ' 6 in

Rupture
2 in < d ≤ 6 in

- Immediate Ignition — Pool/Torch Fire
- Delayed Ignition
  - Fire
    - Flash Fire
    - Vapor Cloud Explosion — VCE
- No Ignition — Toxic Cloud

Major Leak
0.25 in < d ≤ 6 in

- Immediate Ignition — Pool/Torch Fire
- Delayed Ignition
  - Fire
    - Flash Fire
    - Vapor Cloud Explosion — VCE
- No Ignition — Toxic Cloud

Minor Leak
d ≤ 0.25 in

- Immediate Ignition — Pool/Torch Fire
- Delayed Ignition
  - Fire
    - Flash Fire
    - Vapor Cloud Explosion — VCE
- No Ignition — Toxic Cloud

Figure 4-2
Event Tree for a Flammable/Toxic Release

QUEST

Figure 4-3
Worst-Case Consequence Analysis Hazard Footprint - NHT (Explosion Overpressure)

QUEST

4.2.3 Flash Fires

A release of flammable fluid, if not ignited immediately, will create a vapor cloud that travels downwind and disperses. The extent of the flammable zone is defined by the lower flammable limit (LFL). If the flammable cloud is ignited after reaching its full extent, the largest possible flash fire will result. The hazard footprint for a rupture of the liquid reflux line leaving the debutanizer overhead accumulator in the NHT is shown in Figure 4-4. This hazard extends 1,090 ft downwind from the point of release. The flash fire hazard zone is similar to the toxic hazard zone in that the vulnerability zone (circle) covers a much larger area than the actual vapor cloud (the hazard footprint represented by the shaded area).
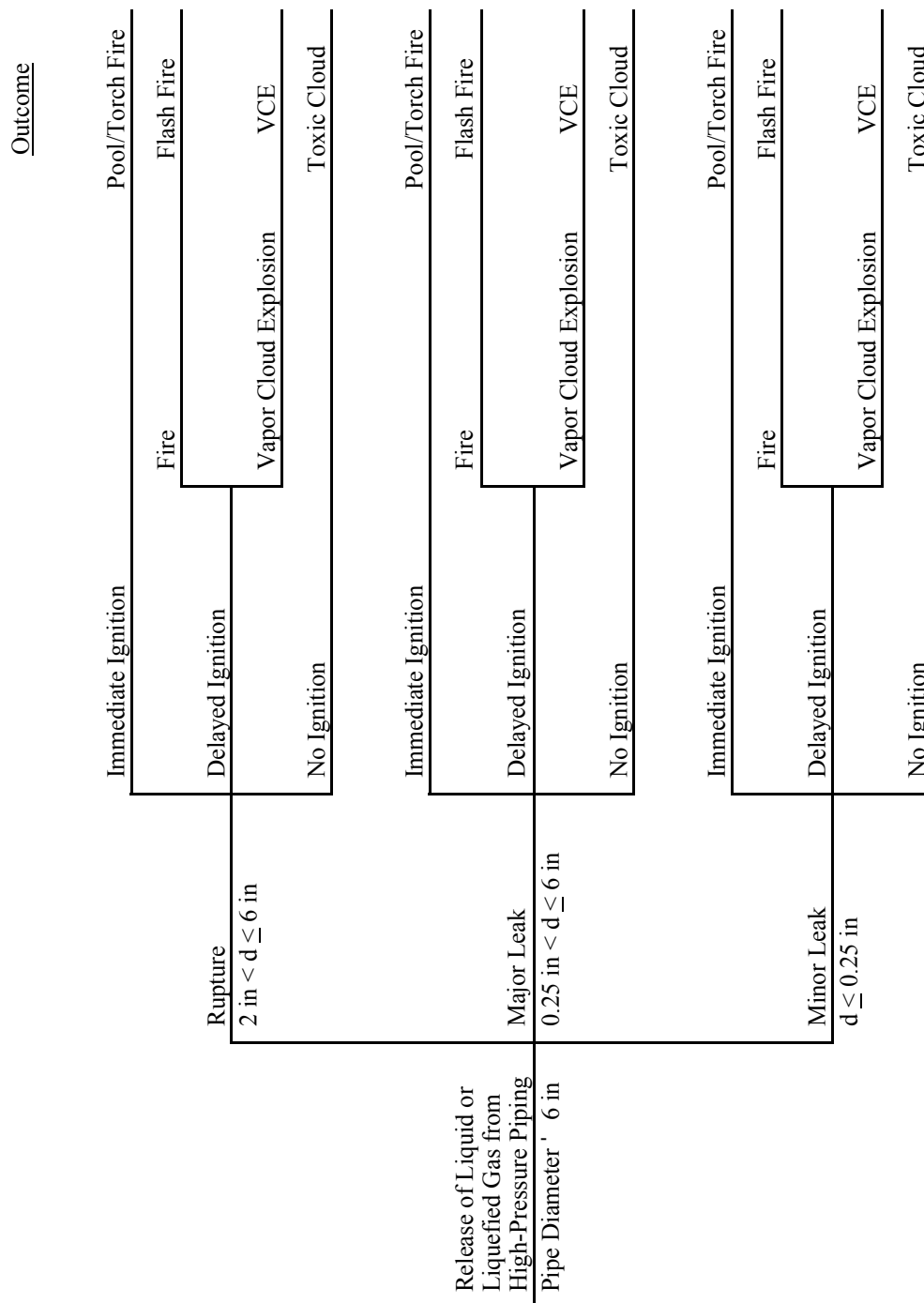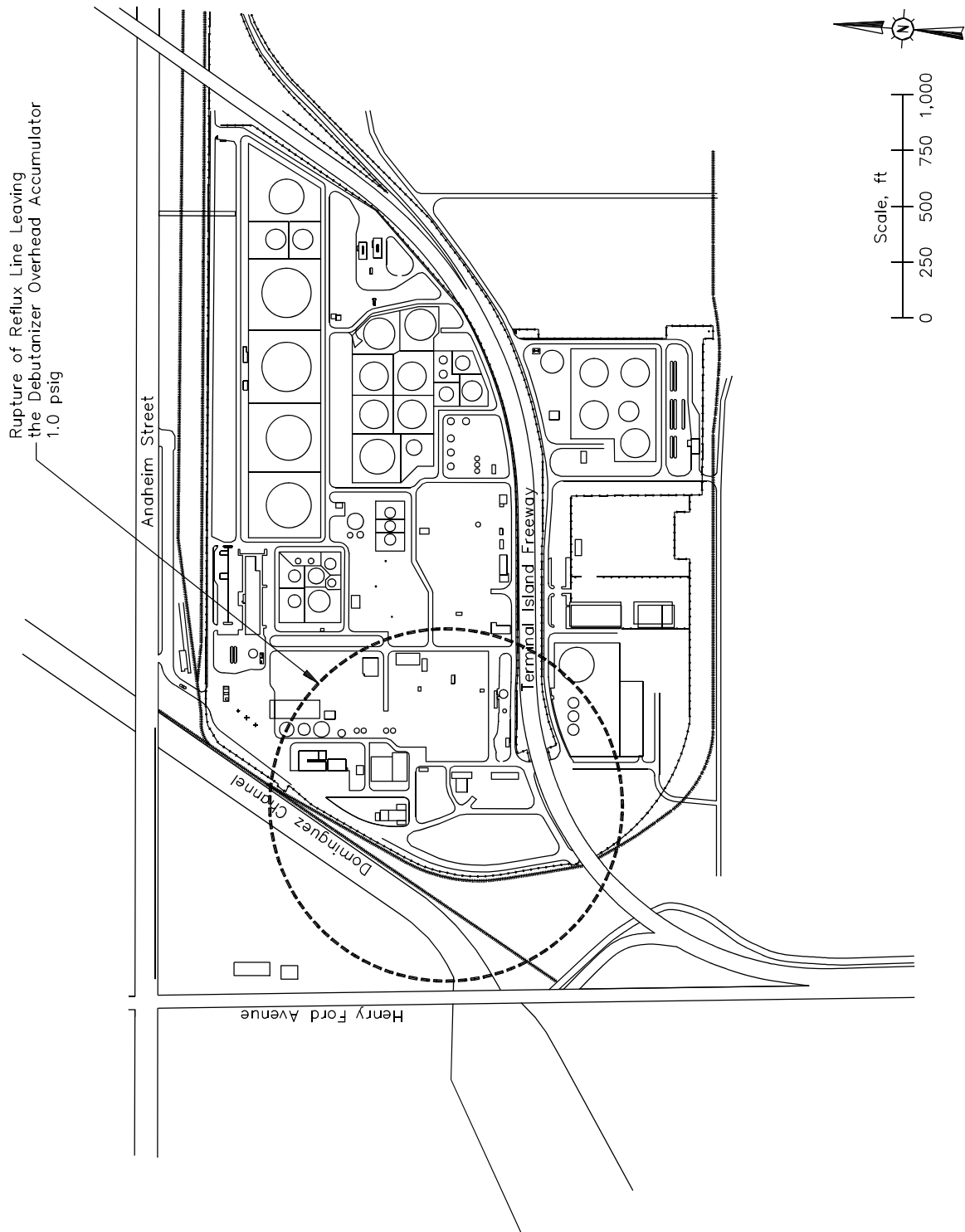
4.2.4 Fire Radiation

The most significant fire radiation hazards that might occur are torch fires from liquefied gas releases. Unlike the dispersion calculations, the worst-case atmospheric conditions for torch fire radiation calculations occur when the winds are high, allowing the flame to "bend" downwind. The largest potential pool fire hazard zones are due to atmospheric storage tank fires. Examples of radiant hazard zones for an immediately ignited rupture of the liquid line leaving the debutanizer overhead accumulator in the NHT, and tank fires from the current and proposed locations of the recovered oil tanks are presented in Figure 4-5.

4.3 Summary of Maximum Hazard Zones

Table 4-2 presents a listing of the type and size of potential hazards which dominate each of the units evaluated. Note that for each unit, the status is defined as E, M, or N (existing, modified, or new). The largest hazards are listed for releases from the existing units and the units after the proposed modifications. The hazards resulting from storage tank fires are listed in Table 4-3. The most significant hazards associated with the pressurized storage tanks (LPG bullets) are BLEVEs. The distance to the thermal radiation endpoint for each size of LPG storage bullet is listed in Table 4-4.

Overall, the proposed additions and modifications result in a limited number of increases in the size of potential hazards. Many of the increases in hazard zones are restricted to Ultramar's property. The addition of two new LPG bullets created the largest increase in radiant off-site hazards, but the effects of bullet BLEVEs (rare events) are constrained to off-site industrial areas.

QUEST
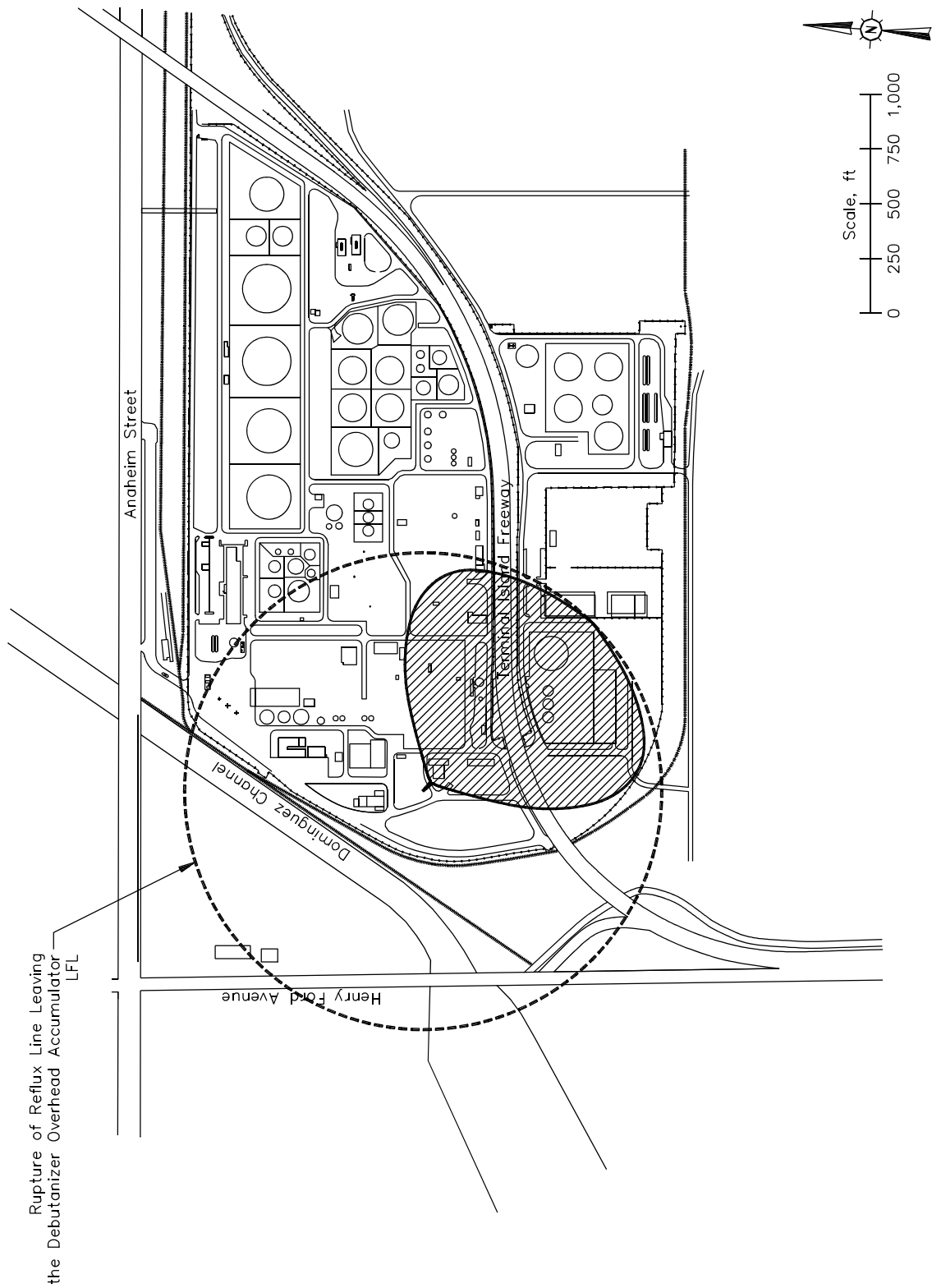
Figure 4-4
Worst-Case Consequence Analysis Hazard Footprint - NHT (Flash Fire)

QUEST
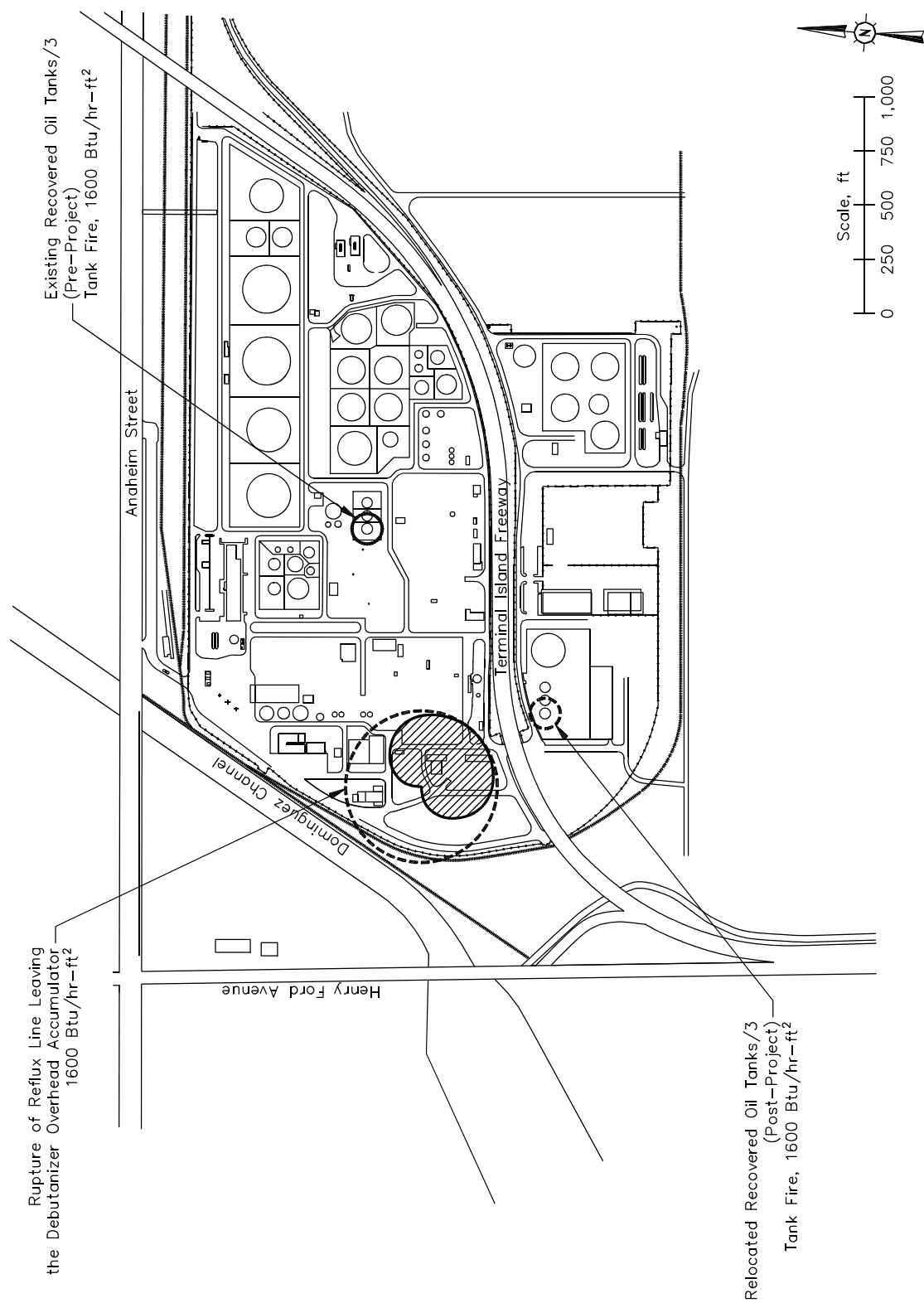
Figure 4-5
Worst-Case Consequence Analysis Hazard Footprints - NHT, TANK (Fire Radiation)

Existing Recovered Oil Tanks/3
(Pre-Project)
Tank Fire, 1600 Btu/hr-ft²

Anaheim Street

Terminal Island Freeway

Dominguez Channel

Henry Ford Avenue

Rupture of Reflux Line Leaving
the Debutanizer Overhead Accumulator
1600 Btu/hr-ft²

Relocated Recovered Oil Tanks/3
(Post-Project)
Tank Fire, 1600 Btu/hr-ft²

Scale, ft
0   250   500   750   1,000

QUEST

Table 4-2

Maximum Hazard Distances for Maximum Credible Event in Each Process Unit/Area

Process Unit/Release	Status of Potential Hazard (E) Existing (M) Modified (N) New	Maximum Distance (ft) from Center of Unit to				
		Flash Fire (LFL)	Explosion Overpressure (1.0 psig)	Pool/Torch Fire Thermal Radiation (1,600 Btu/(hr·ft²))	H₂S Gas Concentration (30 ppm for 60 min)	HF Gas Concentration (20 ppm for 60 min)
LER1						
Release from sour gas line leaving absorber	E	80	60	100	1,280	
	M	80	60	100	1,130	
Release from sour gas line leaving debutanizer accumulator	E	280	200	80	1,510	
	M	290	200	80	990	
Release from debutanizer accumulator liquid	E	640	440	150		
	M	620	440	160	1,820	
Release from depropanizer bottoms	E	500	430	200	500	
	M	570	490	210	570	
LER2						
Release from sour gas line leaving absorber	E	80	60	100	1,290	
	M	80	60	100	1,140	
Release from sour gas line leaving debutanizer accumulator	E	230	180	90	1,650	
	M	310	250	110	2,330	
Release from debutanizer accumulator liquid	E	760	600	240	2,880	
	M	770	610	230	3,350	
Release from depropanizer bottoms	E	1,020	750	400		
	M	1,130	830	410		

QUEST

Table 4-2
Maximum Hazard Distances for Maximum Credible Event in Each Process Unit/Area
(Continued)

Process Unit/Release	Status of Potential Hazard (E) Existing (M) Modified (N) New	Maximum Distance (ft) from Center of Unit to				
		Flash Fire (LFL)	Explosion Overpressure (1.0 psig)	Pool/Torch Fire Thermal Radiation (1,600 Btu/(hr@²))	H_2S Gas Concentration (30 ppm for 60 min)	HF Gas Concentration (20 ppm for 60 min)
NHT						
Release from reactor effluent line	E	230	170	360	1,320	
	M	230	180	350	880	
Release from stripper bottoms	E	1,200	1,010	480		
	M	1,290	1,090	470		
Release from naphtha stripper bottoms	E	1,380	990	590		
	M	1,300	950	590		
Release from splitter overhead accumulator	E	1,940	1,220	450		
	M	1,770	1,160	470		
Release of sour gas from stripper overhead accumulator	E	90	60	110	1,530	
	M	80	60	100	1,310	
Release from debutanizer reflux line	N	1,090	790	350	2,150	
MEROX						
Release of LPG from caustic prewash vessel	E	1,030	620	170		
	M	1,270	820	220		

QUEST

Table 4-2
Maximum Hazard Distances for Maximum Credible Event in Each Process Unit/Area
(Continued)

Process Unit/Release	Status of Potential Hazard (E) Existing (M) Modified (N) New	Maximum Distance (ft) from Center of Unit to				
		Flash Fire (LFL)	Explosion Overpressure (1.0 psig)	Pool/Torch Fire Thermal Radiation (1,600 Btu/(hr·ft²))	H₂S Gas Concentration (30 ppm for 60 min)	HF Gas Concentration (20 ppm for 60 min)
ALKY Release from settler acid outlet	E					25,240
	M					18,850
Release from olefin feed to reactor #2	E	1,960	1,300	360		
	M	1,960	1,300	360		
Release from reactor #2 outlet	E	90	110	190		24,790
	M	50	60	150		20,570
Release from isostripper bottoms	E	1,320	1,060	770		
	M	1,380	1,100	770		
Release from depropanizer receiver outlet	E	1,090	910	440		
	M	1,170	970	440		
Release from recontactor acid line	N					5,540
FGTU Release from fuel gas inlet	E	120	90	150	210	
	M	120	90	150	210	
BUTAMER Release from feed surge drum	E	1,180	830	400		
	M	1,280	890	410		
Release from stabilizer bottoms	E	830	670	270		
	M	960	750	290		
Release from debutanizer overhead accumulator	E	1,750	1,400	595		
	M	1,960	1,570	590		

QUEST

Table 4-2

Maximum Hazard Distances for Maximum Credible Event in Each Process Unit/Area

(Continued)

Process Unit/Release		Status of Potential Hazard (E) Existing (M) Modified (N) New	Maximum Distance (ft) from Center of Unit to				
			Flash Fire (LFL)	Explosion Overpressure (1.0 psig)	Pool/Torch Fire Thermal Radiation (1,600 Btu/(hr@⁴))	H$_2$S Gas Concentration (30 ppm for 60 min)	HF Gas Concentration (20 ppm for 60 min)
LPG (C4 STORAGE)	Release from butane sphere	E	2,450	5,490	2,485		
		M	2,510	7,880	2,530		
LPG (C3 STORAGE)	Release from propane bullet	E	2,010	5,300	2,175		
		M	2,250	5,640	2,685		
BOILER	Release from boiler fuel gas line	N	90	70	80		
AQNH3 TANK	Release from aqueous NH$_3$ tank	E				210	
		M				300	
HOH	Release from fuel gas line	E	80	60	70		
		M	90	70	80		

QUEST

Table 4-3
Maximum Hazard Distances from Fires in Modified or New Atmospheric Storage Tanks

Tank Number	Status of Potential Hazard (E) Existing (M) Modified (N) New	Tank Contents	Distance (ft) from Center of Tank to 1,600 Btu/(hr@ft^2)
95-TK-1	E	Recovered oil	70
95-TK-950 95-TK-752	M	Recovered oil	70

Table 4-4
Maximum Hazard Distances from LPG Bullet BLEVEs

Tank Number	Status of Potential Hazard (E) Existing (M) Modified (N) New	Tank Capacity (barrels)	Distance (ft) from Center of Tank to 1,600 Btu/(hr@ft^2)
82-V-1 (C$_3$)	E	2,000	2,175
82-V-23 (C$_3$)	N	4,000	2,685
81-V-8 (C$_4$)	E	4,760	2,485
81-V-9 (C$_4$)	N	5,000	2,530

QUEST

SECTION 5
CONCLUSIONS

The primary conclusion that can be drawn from the worst-case consequence modeling results is that for the new process unit, the proposed modifications to existing process units and the additions to storage do not result in significantly larger potential hazard zones than those posed by the existing Ultramar Refinery configuration. This result is primarily due to the nature of many of the modifications, which can best be described in the following manner.

- Modification of a unit such that the largest potential hazard is changed only slightly (e.g., Butamer Unit).
- Addition of equivalent equipment such that the potential hazards are essentially the same as those which already exist (e.g., the Merox Unit).
- Relocating products within the refinery property (e.g., relocating atmospheric storage tanks, the hazards associated with atmospheric storage of liquid hydrocarbons remain the same and remain on-site).

With the maximum hazard zones defined for each release, the units can be divided into three categories, dependent on their potential to impact the public. The categories are defined as:

- Units with no potential pre- or post-project off-site impacts (hazard zones are contained on-site).
    HOH
    BOILER
    FGTU
    TANK
    AQNH3 TANK
- Units with potential pre- or post-project off-site impacts, but post-project impacts are no larger than pre-project (existing) impacts.
    ALKY
- Units with potential off-site impacts. Post-project impacts are larger than pre-project impacts.
    LER1
    LER2
    NHT
    MEROX
    BUTAMER
    LPG (C4 STORAGE)
    LPG (C3 STORAGE)

Two specific conclusions can be drawn from a review of the worst-case consequence modeling results. First, for those units where post-project off-site impacts are larger then pre-project off-site impacts, none of the increased hazard zones reach a residential area. All are confined to the industrial area near the Ultramar refinery complex. The worst-case comparison is only valid for the maximum impact distances. All other potential releases are smaller and, in many cases, there is no difference between the pre- and post-project impacts.

The second specific conclusion that can be drawn from the study is that the modifications to the Alkylation Unit (ALKY) produce a significant reduction in the potential worst-case impact following a release of hydrofluoric acid bearing fluids. The implementation of the ReVAP process, with its use of the acid additive which reduces the volatility of the acid phase, results in an 18.5% reduction in the maximum hazard distance.

QUEST

Similar reductions in the downwind travel of HF-bearing clouds will be found for all potential acid releases in the proposed alkylation unit.

None of the modified or new units creates a new hazard that could extend into residential areas. With the exception of the Alkylation Unit; all off-site hazards are confined to industrial areas surrounding the facility. The potential impacts from the Alkylation Unit are significantly reduced with the use of the ReVAP process. Although there is still the potential for a release to extend off-site into residential areas, the area potentially exposed will be reduced with the project modifications. It should be kept in mind that for the worst-case scenario to occur, the following conditions must be met.

(1)   A full rupture of the line occurs.
(2)   The release does not ignite within minutes of the rupture.
(3)   The wind speed is low (less than 3 mph).
(4)   The atmosphere is calm.

This sequence of events is highly unlikely and only results in an off-site hazard (toxic or flammable vapor dispersion) for a limited number of potential releases. The other hazards that were found to be larger after the proposed additions and modifications were a BLEVE of one of the new LPG bullets. These events, which are not affected by the above considerations, are also very rare.

QUEST

SECTION 6
REFERENCES

AIHA (1988), *Emergency Response Planning Guidelines*. American Industrial Hygiene Association, Akron, Ohio, 1988.

Chang, Joseph C., Mark E. Fernau, Joseph S. Scire, and David G. Strimatis (1998), *A Critical Review of Four Types of Air Quality Models Pertinent to MMS Regulatory and Environmental Assessment Missions*. Mineral Management Service, Gulf of Mexico OCS Region, U.S. Department of the Interior, New Orleans, November, 1998.

EPA (1996), *Accidental Release Prevention Requirements: Risk Management Programs Under the Clean Air Act, Section 112(r)(7)*. Environmental Protection Agency, 40 CFR Part 68, 1996.

Hanna, S. R., D. G. Strimaitis, and J. C. Chang (1991), *Hazard Response Modeling Uncertainty (A Quantitative Method), Volume II, Evaluation of Commonly-Used Hazardous Gas Dispersion Models*. Study cosponsored by the Air Force Engineering and Services Center, Tyndall Air Force Base, Florida, and the American Petroleum Institute; performed by Sigma Research Corporation, Westford, Massachusetts, September, 1991.

TRC (1991), *Evaluation of Dense Gas Simulation Models*. Prepared for the U.S. Environmental Protection Agency by TRC Environmental Consultants, Inc., East Hartford, Connecticut 06108, EPA Contract No. 68-02-4399, May, 1991.

QUEST

SECTION 7
GLOSSARY

The following definitions are intended to apply to Consequence Analysis and Quantitative Risk Analysis studies of facilities that produce, process, store, or transport hazardous materials. Due to the limited scope of such studies, some of these definitions are more narrow than the common definitions.

ACCIDENT. An unplanned event that interrupts the normal progress of an activity and has undesirable consequences, and is preceded by an unsafe act and/or an unsafe condition.

ACCIDENT EVENT SEQUENCE. A specific series of unplanned events that has specific undesirable consequences (e.g., a pipe ruptures, allowing flammable gas to escape; the gas forms a flammable vapor cloud that ignites after some delay, resulting in a flash fire).

ACCIDENT SCENARIO. The detailed description of an accident event sequence.

AIR DISPERSION MODELING. The use of mathematical equations (models) to predict the rate at which vapors or gases released into the air will be diluted (dispersed) by the air. The purpose of air dispersion modeling is to predict the extent of potentially toxic or flammable gas concentrations, in air, by calculating the change in concentration of the vapor or gas in the air as a function of distance from the source of the vapor or gas.

BLAST WAVE. An atmospheric pressure pulse created by an explosion.

BLEVE (Boiling Liquid–Expanding Vapor Explosion). The sudden, catastrophic failure of a pressure vessel at a time when its liquid contents are well superheated. (BLEVE is normally associated with the rupture, due to fire impingement, of pressure vessels containing liquefied gases.)

CONDITIONAL PROBABILITY. The probability of occurrence of an event, given that one or more precursor events have occurred (e.g., the probability of ignition of an existing vapor cloud).

CONSEQUENCES. The expected results of an incident outcome.

CONSEQUENCE ANALYSIS. Selection and definition of specific accident event sequences, coupled with consequence modeling.

CONSEQUENCE MODELING. The use of mathematical models to predict the potential extent of specific hazard zones or effect zones that would result from specific accident event sequences.

DEFLAGRATION. See explosion.

DETONATION. See explosion.

EFFECT ZONE. The area over which the airborne gas concentration, radiant heat flux, or blast wave overpressure is predicted to equal or exceed some specified value. In contrast to a hazard zone, the endpoint for an effect zone need not be capable of producing injuries or damage.

QUEST

ENDPOINT. The specified value of airborne gas concentration, radiant heat flux, or blast wave overpressure used to define the outer boundary of an effect zone or hazard zone. Endpoints typically correspond to specific levels of concern (e.g., IDLH, LFL, onset of fatality, 50% mortality, odor threshold, etc.).

EVENT TREE. A diagram that illustrates accident event sequences. It begins with an initiating event (e.g., a release of hydrogen sulfide gas), passes through one or more intermediate events (e.g., ignition or no ignition), resulting in two or more incident outcomes (e.g., flash fire or toxic vapor cloud).

EXPLOSION. A rapid release of energy, resulting in production of a blast wave. There are two common types of explosions—physical explosions (sudden releases of gas or liquefied gas from pressurized containers) and chemical explosions (rapid chemical reactions, including rapid combustion). Chemical explosions can be further subdivided into deflagrations and detonations. In a deflagration, the velocity of the blast wave is lower than the speed of sound in the reactants. In a detonation, the velocity of the blast wave exceeds the speed of sound in the reactants. For a given mass of identical reactants, a detonation is capable of producing more damage than a deflagration. Solid and liquid explosives, such as dynamite and nitroglycerine, typically detonate, whereas vapor cloud explosions are nearly always deflagrations.

FIRE RADIATION. See thermal radiation.

FLAMMABLE VAPOR CLOUD. A vapor cloud consisting of flammable gas and air, within which the gas concentration equals or exceeds its lower flammable limit.

FLASH FIRE. Transient combustion of a flammable vapor cloud.

HAZARD. A chemical or physical condition that presents a potential for causing injuries or illness to people, damage to property, or damage to the environment.

HAZARD ZONE. The area over which a given incident outcome is capable of producing undesirable consequences (e.g., skin burns) that are equal to or greater than some specified injury or damage level (e.g., second-degree skin burns). (Sometimes referred to as a "hazard footprint.")

INCIDENT OUTCOME. The result of an accident event sequence. The incident outcomes of interest in a typical study are toxic vapor clouds; fires (flash fire, torch fire, pool fire, or fireball); and explosions (confined, unconfined, or physical).

INITIATING EVENT. The first event in an accident event sequence. Typically a failure of containment (e.g., gasket failure, corrosion hole in a pipe, hose rupture, etc.).

INTERMEDIATE EVENT. An event that propagates or mitigates the previous event in an accident event sequence (e.g., operator fails to respond to an alarm, thus allowing a release to continue; excess flow valve closes, thus stopping the release).

ISOPLETH. The locus of points at which a given variable has a constant value. In consequence modeling, the variable can be airborne gas concentration, radiant heat flux, or blast wave overpressure. The value of the variable is equal to the specified endpoint. The area bounded by an isopleth is an effect zone.

LOWER FLAMMABLE LIMIT. The lowest concentration of flammable gas in air that will support flame propagation.

QUEST

MISSILES. See shrapnel.

POOL FIRE. Continuous combustion of the flammable gas emanating from a pool of liquid.

QUANTITATIVE RISK ANALYSIS. The development of a quantitative estimate of risk based on engineering evaluation and mathematical techniques for combining estimates of incident consequences and frequencies.

RISK. A measure of economic loss or human injury in terms of both the incident likelihood and the magnitude of the loss or injury.

RISK ASSESSMENT. The process by which the results of a risk analysis are used to make decisions, either through relative ranking of risk reduction strategies or through comparison with risk targets.

SHRAPNEL. Solid objects projected outward from the source of an explosion. Sometimes referred to as missiles or projectiles.

SUPERHEATED LIQUID. A liquid at a temperature greater than its atmospheric pressure boiling point.

THERMAL RADIATION. The transfer of heat by electromagnetic waves. This is how heat is transferred from flames to an object or person not in contact with or immediately adjacent to the flames. This is also how heat is transferred from the sun to the earth.

TORCH FIRE. Continuous combustion of a flammable fluid that is being released with considerable momentum.

TOXIC. Describes a material with median lethal doses and/or median lethal concentrations listed in OSHA 29 CFR 1910.1200, Appendix A.

TOXIC VAPOR CLOUD. A vapor cloud consisting of toxic gas and air, within which the gas concentration equals or exceeds a concentration that could be harmful to humans exposed for a specific time.

VAPOR CLOUD. A volume of gas/air mixture within which the gas concentration equals or exceeds some specified or defined concentration limit.

VAPOR CLOUD EXPLOSION. Extremely rapid combustion of a flammable vapor cloud, resulting in a blast wave.

VULNERABILITY ZONE. The area within the circle created by rotating a hazard zone around its point of origin. Any point within that circle could, under some set of circumstances, be exposed to a hazard level that equals or exceeds the endpoint used to define the hazard zone. However, except for accidents that produce circular hazard zones (e.g., BLEVEs and confined explosions), only a portion of the area within the vulnerability zone can be affected by a single accident.

QUEST

API	American Petroleum Institute
BLEVE	Boiling Liquid–Expanding Vapor Explosion
CCPS	Center for Chemical Process Safety
DOT	Department of Transportation
EPA	Environmental Protection Agency
ESD	Emergency Shut Down
FTA	Fault Tree Analysis
IDLH	Immediately Dangerous to Life or Health
LFL	Lower Flammable Limit
LPG	Liquefied Petroleum Gas
NFPA	National Fire Protection Association
OREDA	Offshore Reliability Data
psig	Pounds per square inch, gauge
QRA	Quantitative Risk Analysis
RMP	Risk Management Plan
STEL	Short-Term Exposure Limit
TNO	Netherlands Organization of Applied Scientific Research (Nederlandse Organisatie voor toegepest-natuurwetenschallelijk onderzoek)
TNT	Trinitrotoluene
USCB	United States Census Bureau
USNRC	United States Nuclear Regulatory Commission

QUEST

APPENDIX A
CANARY BY QUEST® MODEL DESCRIPTIONS

The following model descriptions are taken from the CANARY by Quest User Manual.

QUEST

Engineering Properties

Purpose

The purpose of this model is to provide an accurate means of computing physical and thermodynamic properties of a wide range of chemical mixtures and pure components using a minimum of initial information.

Required Data

(a)   Fluid composition
(b)   Temperature and pressure of the fluid prior to release

Methodology

Basic thermodynamic properties are computed using the Peng-Robinson equation of state [Peng and Robinson, 1976]. The necessary physical and thermodynamic properties are calculated in the following manner.

Step 1: The temperature and pressure of the fluid at storage conditions and the identity and mole fraction of each component of the fluid are obtained. Mixture parameters are determined using data from the extensive properties data base within CANARY.

Step 2: Each calculation begins with the computation of the vapor and liquid fluid composition. For cases where the temperature and pressure result in only one phase being present, the vapor or liquid composition will be the same as the initial feed composition. The composition calculation is an iterative procedure using a modification of the techniques described by Starling [1973].

Step 3: Once the vapor and liquid compositions are known, the vapor and liquid densities, enthalpies, entropies, and heat capacities can be computed directly. Other physical properties (viscosity, thermal conductivity, surface tension, etc.) are computed using correlations developed in Reid, Prausnitz, and Poling [1987].

Step 4: A matrix of properties is computed over a range of temperatures and pressures. Physical and thermodynamics properties required by other models within CANARY are then interpolated from this table.

Basic Thermodynamic Equations

$$Z^3 - (1-B) \cdot Z^2 + \left(A - 3 \cdot B^2 - 2 \cdot B\right) \cdot Z - \left(A \cdot B - B^2 - B^3\right) = 0 \tag{1}$$

where: Z = fluid compressibility factor, $\dfrac{P \cdot V}{R \cdot T}$, dimensionless

P = system pressure, kPa

V = fluid specific volume, m³/kmol

R = gas constant, 8.314 m³·kPa/(kmol·K)

T = absolute temperature, K

$A = \dfrac{a \cdot P}{R^2 \cdot T^2}$

$a = 0.45724 \cdot \dfrac{R^2 \cdot T^2}{P_c} \cdot \alpha$

$\alpha = \left[1 + m \cdot \left(1 - T_r^{0.5} \right)^2 \right]$

$m = 0.37464 + 1.54226 \cdot \omega - 0.26992 \cdot \omega^2$

ω = acentric factor

$T_r = \dfrac{T}{T_c}$

T_c = pseudo-critical temperature, K

P_c = pseudo-critical pressure, kPa

$B = \dfrac{b \cdot P}{R \cdot T}$

$b = 0.0778 \cdot R \cdot \dfrac{T_c}{P_c}$

$$H = H^o + \frac{P}{\rho} - R \cdot T + \int_0^{\rho} \left[P - T \cdot \left(\frac{\partial P}{\partial T} \right)_{\rho} \right] \cdot \left(\frac{d\rho}{\rho^2} \right) \tag{2}$$

where: H = enthalpy of fluid at system conditions, kJ/kg

H^o = enthalpy of ideal gas at system temperature, kJ/kg

$$S = S^o - R \cdot \ln\left(\rho \cdot R \cdot T \right) + \int_0^{\rho} \left[\rho \cdot R - \left(\frac{\partial P}{\partial T} \right)_{\rho} \right] \cdot \left(\frac{d\rho}{\rho^2} \right) \tag{3}$$

where: S = entropy of fluid at system conditions, kJ/(kg·K)

S^o = entropy of ideal gas at system temperature, kJ/(kg·K)

$$R \cdot T \cdot \ln\left(\frac{f_i}{f_i^o} \right) = \left[\left(H_i - H_i^o \right) - T \cdot \left(S_i - S_i^o \right) \right] \tag{4}$$

where: f_i = fugacity of component i, kPa

f_i^o = standard state reference fugacity, kPa

References

Peng, D., and D. B. Robinson, "New Two-Constant Equation of State." *Industrial Engineering Chemistry Fundamentals*, Vol. 15, No. 59, 1976.

Reid, R. C., J. M. Prausnitz, and B. E. Poling, *The Properties of Gases and Liquids* (Fourth Edition). McGraw-Hill Book Company, New York, New York, 1987.

Starling, K. E., *Fluid Thermodynamic Properties for Light Petroleum Systems*. Gulf Publishing Company, Houston, Texas, 1973.

Pool Fire Radiation Model

Purpose

The purpose of this model is to predict the impact of fire radiation emitted by flames that are fueled by vapors emanating from liquid pools. Specifically, the model predicts the maximum radiant heat flux incident upon a target as a function of distance between the target and the flame.

Required Data

(a)   Composition of the liquid in the pool
(b)   Temperature of the liquid in the pool
(c)   Wind speed
(d)   Air temperature
(e)   Relative humidity
(f)   Elevation of the target (relative to grade)
(g)   Elevation of the pool (relative to grade)
(h)   Dimensions of the free surface of the pool
(i)   Orientation of the pool (relative to the wind direction)
(j)   Spill surface (land or water)

Methodology

Step 1: The geometric shape of the flame is defined. The flame column above a circular pool, square pool, or rectangular pool is modeled as an elliptical cylinder.

Step 2: The dimensions of the flame column are determined. The dimensions of the base of the flame are defined by the pool dimensions. An empirical correlation developed by Thomas [1965] is used to calculate the length (height) of the flame.

$$L = 42 \cdot D_h \cdot \left(\frac{\dot{m}}{\rho_a \cdot \left(g \cdot D_h \right)^{0.5}} \right)^{0.61}$$

where: L = length (height) of the flame, m
D_h = hydraulic diameter of the liquid pool, m
$\dot{m}$ = mass burning flux, kg/(m$^2 \cdot$ s)
ρ_a = density of air, kg/m^3
g = gravitational acceleration, 9.8 m/s^2

Notes: Mass burning fluxes used in the Thomas equation are the steady-state rates for pools on land (soil, concrete, etc.) or water, whichever is specified by the user.

For pool fires with hydraulic diameters greater than 100 m, the flame length, L, is set equal to the length calculated for $D_h = 100$ m.

Step 3: The angle (Φ) to which the flame is bent from vertical by the wind is calculated using an empirical correlation developed by Welker and Sliepcevich [1970].

$$\frac{\tan(\Phi)}{\cos(\Phi)} = 3.2 \cdot \left(\frac{D_h \cdot u \cdot \rho_a}{\mu_a} \right)^{0.07} \cdot \left(\frac{u^2}{g \cdot D_h} \right)^{0.7} \cdot \left(\frac{\rho_v}{\rho_a} \right)^{-0.6}$$

where: Φ = angle the flame tilts from vertical, degrees

u = wind speed, m/s

μ_a = viscosity of air, kg/(m·s)

ρ_v = density of fuel vapor, kg/m³

Step 4: The increase in the downwind dimension of the base of the flame (flame drag) is calculated using a generalized form of the empirical correlation Moorhouse [1982] developed for large circular pool fires.

$$D_w = 1.5 \cdot D_x \cdot \left(\frac{u^2}{g \cdot D_x} \right)^{0.069}$$

where: D_w = downwind dimension of base of tilted flame, m

D_x = downwind dimension of the pool, m

Step 5: The flame is divided into two zones: a clear zone in which the flame is not obscured by smoke; and a smoky zone in which a fraction of the flame surface is obscured by smoke. The length of the clear zone is calculated by the following equation, which is based on an empirical correlation developed by Pritchard and Binding [1992].

$$L_c = 55.05 \cdot D_h^{-0.6} \cdot \left(\frac{\dot{m}}{\rho_a} \right)^{1.13} \cdot (u+1)^{0.179} \cdot \left(\frac{C}{H} \right)^{-2.49}$$

where: L_c = length of the clear zone, m

$\dfrac{C}{H}$ = carbon/hydrogen ratio of fuel, dimensionless

Step 6: The surface flux of the clear zone is calculated using the following equation.

$$q_{cz} = q_{sm} \cdot \left(1 - e^{-b \cdot D_h} \right)$$

where: q_{cz} = surface flux of the clear zone, kW/m²

q_{sm} = maximum surface flux, kW/m²

b = extinction coefficient, m⁻¹

Average surface flux of the smoky zone, q_{sz}, is then calculated, based on the following assumptions.

- The smoky zone consists of clean-burning areas and areas in which the flame is obscured by smoke.
- Within the smoky zone, the fraction of the flame surface that is obscured by smoke is a function of the fuel properties and pool diameter.
- Smoky areas within the smoky zone have a surface flux of 20 kW/m² [Hagglund and Persson,1976].
- Clean-burning areas of the smoky zone have the same surface flux as the clean-burning zone.
- The average surface flux of the smoky zone is the area-weighted average of the surface fluxes for the smoky areas and the clean-burning areas within the smoky zone.

(This two-zone concept is based on the Health and Safety Executive POOLFIRE6 model, as described by Rew and Hulbert [1996].)

Step 7: The surface of the flame is divided into numerous differential areas. The following equation is then used to calculate the view factor from a differential target, at a specific location outside the flame, to each differential area on the surface of the flame.

$$F_{dA_t \to dA_f} = \frac{\cos(\beta_t) \cdot \cos(\beta_f)}{\pi \cdot r^2} \cdot dA_f \qquad \text{for } [\,\beta_t\,] \text{ and } [\,\beta_f\,] < 90°$$

where: $F_{dA_t \to dA_f}$ = view factor from a differential area on the target to a differential area on the surface of the flame, dimensionless
dA_f = differential area on the flame surface, m²
dA_t = differential area on the target surface, m²
r = distance between differential areas dA_t and dA_f, m
β_t = angle between normal to dA_t and the line from dA_t to dA_f, degrees
β_f = angle between normal to dA_f and the line from dA_t to dA_f, degrees

Step 8: The radiant heat flux incident upon the target is computed by multiplying the view factor for each differential area on the flame by the appropriate surface flux $(q_{cz}$ or $q_{sz})$ and by the appropriate atmospheric transmittance, then summing these values over the surface of the flame.

$$q_{ai} = \sum_{A_f} q_{sf} \cdot F_{dA_t \to dA_f} \cdot \tau$$

where: q_{ai} = attenuated radiant heat flux incident upon the target due to radiant heat emitted by the flame, kW/m²
A_f = area of the surface of the flame
q_{sf} = radiant heat flux emitted by the surface of the flame, kW/m² (q_{sf} equals either q_{cz} or q_{sz}, as appropriate)
τ = atmospheric transmittance, dimensionless

Atmospheric transmittance, τ, is a function of absolute humidity and r, the path length between differential areas on the flame and target [Wayne, 1991].

Step 9: Steps 7 and 8 are repeated for numerous target locations.

Validation

Several of the equations used in the Pool Fire Radiation Model are empirical relationships based on data from medium- to large-scale experiments, which ensures reasonably good agreement between model predictions and experimental data for variables such as flame length and tilt angle. Comparisons of experimental data and model predictions for incident heat flux at specific locations are more meaningful and of greater interest. Unfortunately, few reports on medium- or large-scale experiments contain the level of detail required to make such comparisons.

One source of detailed test data is a report by Welker and Cavin [1982]. It contains data from sixty-one pool fire tests involving commercial propane. Variables that were examined during these tests include pool size (2.7 to 152 m^2) and wind speed. Figure B-1 compares the predicted values of incident heat flux with experimental data from the sixty-one pool fire tests.
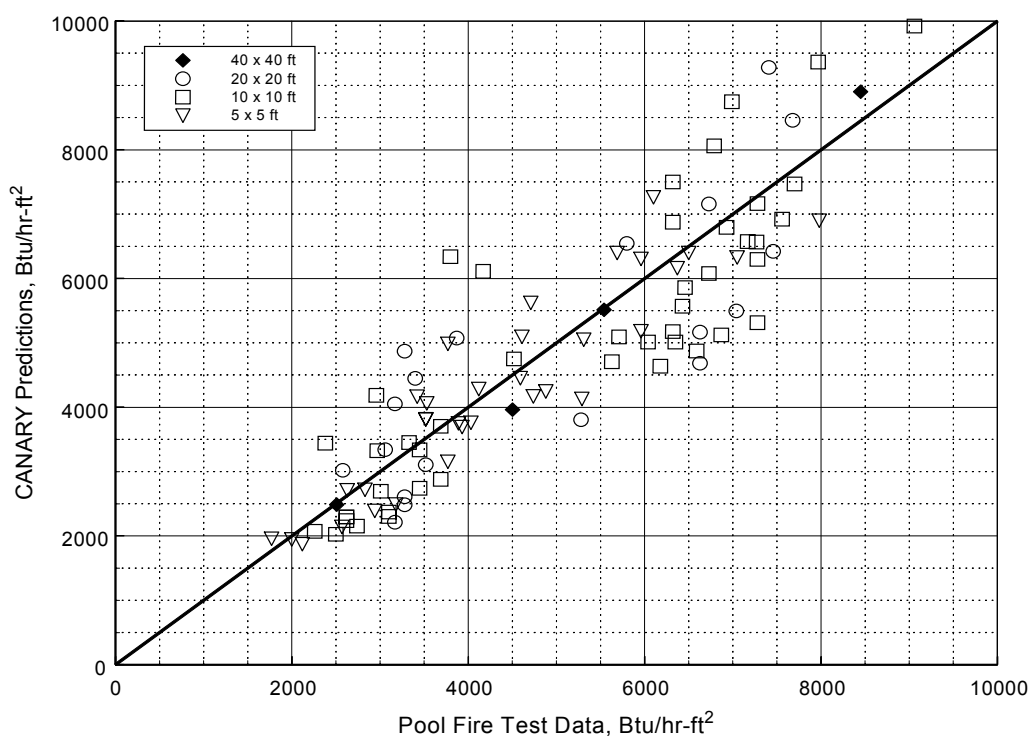

Figure B-1

References

Hagglund B., and L. Persson, *The Heat Radiation from Petroleum Fires*. FOA Rapport, Forsvarets Forskningsanstalt, Stockholm, Sweden, 1976.

Moorhouse, J., "Scaling Criteria for Pool Fires Derived from Large-Scale Experiments." *The Assessment of Major Hazards*, Symposium Series No. 71, The Institution of Chemical Engineers, Pergamon Press Ltd., Oxford, United Kingdom, 1982: pp. 165-179.

Pritchard, M. J., and T. M. Binding, "FIRE2: A New Approach for Predicting Thermal Radiation Levels from Hydrocarbon Pool Fires." *IChemE Symposium Series*, No. 130, 1992: pp. 491-505.

Rew, P. J., and W. G. Hulbert, *Development of Pool Fire Thermal Radiation Model*. HSE Contract Research Report No. 96/1996.

Thomas, P. H., *F.R. Note 600*, Fire Research Station, Borehamwood, England, 1965.

Wayne, F. D., "An Economical Formula for Calculating Atmospheric Infrared Transmissivities." *Journal of Loss Prevention in the Process Industries*, Vol. 4, January, 1991: pp. 86-92.

Welker, J. R., and W. D. Cavin, *Vaporization, Dispersion, and Radiant Fluxes from LPG Spills*. Final Report No. DOE-EP-0042, Department of Energy Contract No. DOE-AC05-78EV-06020-1, May, 1982 (NTIS No. DOE-EV-06020-1).

Welker, J. R., and C. M. Sliepcevich, *Susceptibility of Potential Target Components to Defeat by Thermal Action*. University of Oklahoma Research Institute, Report No. OURI-1578-FR, Norman, Oklahoma, 1970.

Torch Fire and Flare Radiation Model

Purpose

The purpose of this model is to predict the impact of fire radiation emitted by burning jets of vapor. Specifically, the model predicts the maximum radiant heat flux incident upon a target as a function of distance between the target and the point of release.

Required Data

(a)   Composition of the released material
(b)   Temperature and pressure of the material before release
(c)   Mass flow rate of the material being released
(d)   Diameter of the exit hole
(e)   Wind speed
(f)   Air temperature
(g)   Relative humidity
(h)   Elevation of the target (relative to grade)
(i)   Elevation of the point of release (relative to grade)
(j)   Angle of the release (relative to horizontal)

Methodology

Step 1: A correlation based on a Momentum Jet Model is used to determine the length of the flame. This correlation accounts for the effects of:

- composition of the released material,
- diameter of the exit hole,
- release rate,
- release velocity, and
- wind speed.

Step 2: To determine the behavior of the flame, the model uses a momentum-based approach that considers increasing plume buoyancy along the flame and the bending force of the wind. The following equations are used to determine the path of the centerline of the flame [Cook, et al., 1987].

$$\Phi_X = \left(\rho_{ja}\right)^{0.5} \cdot \overline{u} \cdot \sin(\theta) \cdot \cos(\varphi) + \left(\rho_\infty\right)^{0.5} \cdot u_\infty \quad \text{(downwind)}$$

$$\Phi_Y = \left(\rho_{ja}\right)^{0.5} \cdot \overline{u} \cdot \sin(\theta) \cdot \sin(\varphi) \quad \text{(crosswind)}$$

$$\Phi_Z = \left(\rho_{ja}\right)^{0.5} \cdot \overline{u} \cdot \cos(\theta) + \left(\rho_\infty\right)^{0.5} \cdot u_b \cdot \frac{(i+1)}{n} \quad \text{(vertical)}$$

where: Φ_{XYZ} = momentum flux in X, Y, Z direction

       ρ_{ja} = density of the jet fluid at ambient conditions, kg/m³

       $\overline{u}$ = average axial velocity of the flame, m/s

       θ = release angle in $X{-}Z$ plane (relative to horizontal), degrees

       φ = release angle in $X{-}Y$ plane (relative to downwind), degrees

       ρ_∞ = density of air, kg/m³

       u_∞ = wind speed, m/s

       ρ_b = density of combustion products, kg/m³

       u_b = buoyancy velocity, m/s

       n = number of points taken along the flame length

These correlations were developed to predict the path of a torch flame when released at various orientations. The model currently does not allow a release angle in a crosswind direction; the release angle is confined to the downwind/vertical plane (i.e., $\varphi = 0$).

Step 3: The angle of flame tilt is defined as the inclination of a straight line between the point of release and the end point of the flame centerline path (as determined in Step 2).

Step 4: The geometric shape of the flame is defined as a frustum of a cone (as suggested by several flare/fire researchers [e.g., Kalghatgi, 1983, Chamberlain, 1987]), but modified by adding a hemisphere to the large end of the frustum. The small end of the frustum is positioned at the point of release, and the centerline of the frustum is inclined at the angle determined in Step 3.

Step 5: The surface emissive power is determined from the molecular weight and heat of combustion of the burning material, the release rate and velocity, and the surface area of the flame.

Step 6: The surface of the flame is divided into numerous differential areas. The following equation is then used to calculate the view factor from a differential target, at a specific location outside the flame, to each differential area on the surface of the flame.

$$F_{dA_t \to dA_f} = \frac{\cos(\beta_t) \cdot \cos(\beta_f)}{\pi \cdot r^2} \cdot dA_f \qquad \text{for } [\,\beta_t\,] \text{ and } [\,\beta_f\,] < 90°$$

where: $F_{dA_t \to dA_f}$ = view factor from a differential area on the target to a differential area on the surface of the flame, dimensionless

       dA_f = differential area on the flame surface, m²

       dA_t = differential area on the target surface, m²

       r = distance between differential areas dA_t and dA_f, m

       β_t = angle between normal to dA_t and the line from dA_t to dA_f, degrees

       β_f = angle between normal to dA_f and the line from dA_t to dA_f, degrees

Step 7: The radiant heat flux incident upon the target is computed by multiplying the view factor for each differential area on the flame by the surface missive power and by the appropriate atmospheric transmittance, then summing these values over the surface of the flame.

$$q_{ai} = \sum_{A_f} q_{sf} \cdot F_{dA_t \to dA_f} \cdot \tau$$

where: q_{ai} = attenuated radiant heat flux incident upon the target due to radiant heat emitted by the flame, kW/m^2

   A_f = area of the surface of the flame

   q_{sf} = radiant heat flux emitted by the surface of the flame, kW/m^2

   τ = atmospheric transmittance, dimensionless

Atmospheric transmittance, τ, is a function of absolute humidity and r, the path length between differential areas on the flame and target [Wayne, 1991].

Step 8: Steps 6 and 7 are repeated for numerous target locations.

Validation

Several of the equations used in the Torch Fire and Flare Radiation Model are empirical relationships based on data from medium- to large-scale experiments, which ensures reasonably good agreement between model predictions and experimental data for variables such as flame tilt angle. Comparisons of experimental data and model predictions for incident heat flux at specific locations are more meaningful and of greater interest. Unfortunately, few reports on medium- or large-scale experiments contain the level of detail required to make such comparisons.

One reasonable source of test data is a report by Chamberlain [1987]. It contains data from seven flare tests involving natural gas releases from industrial flares, with several data points being reported for each test. Variables that were examined during these tests include release diameter (0.203 and 1.07 m), release rate and velocity, and wind speed. Figure C-1 compares the predicted values of incident heat flux with experimental data from the seven flare tests.

References

Chamberlain, G. A., "Developments in Design Methods for Predicting Thermal Radiation from Flares." *Chemical Engineering Research and Design*, Vol. 65, July, 1987.

Cook, D. K., M. Fairweather, G. Hankinson, and K. O'Brien, "Flaring of Natural Gas from Inclined Vent Stacks." *IChemE Symposium Series #102*, Pergamon Press, 1987.

Kalghatgi, G. T., "The Visible Shape and Size of a Turbulent Hydrocarbon Jet Diffusion Flame in a Cross Wind." *Combustion and Flame*, Vol. 52, 1983: pp. 91-106.

Wayne, F. D., "An Economical Formula for Calculating Atmospheric Infrared Transmissivities." *Journal of Loss Prevention in the Process Industries*, Vol. 4, January, 1991: pp. 86-92.
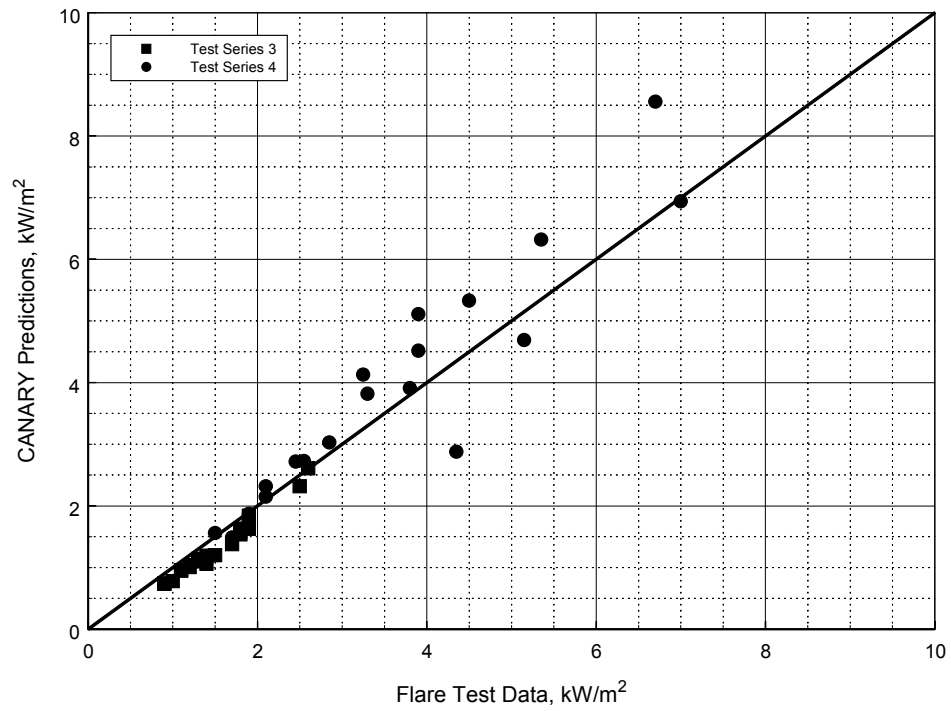
Figure C-1

Fireball Model

Purpose

The purpose of the Fireball Model is to predict the impact of thermal radiation emitted by fireballs that result from catastrophic failures of pressure vessels containing superheated liquids. Specifically, the model predicts the average radiant heat flux incident upon a grade-level target as a function of the horizontal distance between the target and the center of the fireball.

Required Data

(a)   Composition of flammable liquid within the pressure vessel
(b)   Mass of flammable liquid within the pressure vessel
(c)   Pressure within vessel just prior to rupture
(d)   Temperature of the liquid within the vessel just prior to rupture
(e)   Air temperature
(f)   Relative humidity

Methodology

Step 1: Calculate the mass of fuel consumed in the fireball. The mass of fuel in the fireball is equal to the smaller of the mass of fuel in the vessel (as specified by the user), or three times the mass of fuel that flashes to vapor when it is released to the atmosphere [Hasegawa and Sato, 1977].

Step 2: Calculate the maximum diameter of the fireball using the empirical correlation from Roberts [1981/82].

$$D_{max} = 5.8 \cdot M_f^{1/3}$$

where: D_{max} = maximum diameter of the fireball, m
M_f = mass of fuel in the fireball, kg

Step 3: Calculate fireball duration using the following empirical correlation [Martinsen and Marx, 1999].

$$t_d = 0.9 \cdot M_f^{1/4}$$

where: t_d = fireball duration, s
M_f = mass of fuel in the fireball, kg

Step 4: Calculate the size of the fireball and its location, as a function of time. The fireball is assumed to grow at a rate that is proportional to the cube root of time, reaching its maximum diameter, D_{max}, at the time of liftoff, $t_d / 3$. During its growth phase, the fireball remains tangent to grade. After liftoff, it rises at a constant rate [Shield, 1994].

Step 5: Estimate the surface flux of the fireball. The fraction of the total available heat energy that is emitted as radiation is calculated using the equation derived by Roberts [1981/82].

$$f = 0.0296 \cdot P^{0.32}$$

where: f = fraction of available heat energy released as radiation, dimensionless
P = pressure in vessel at time of rupture, kPa

The total amount of energy emitted as radiation is then calculated.

$$E_r = f \cdot M_f \cdot \Delta H_c$$

where: E_r = energy emitted as radiation, kJ
ΔH_c = heat of combustion, kJ/kg

The surface flux is estimated by dividing E_r by the average surface area of the fireball and the fireball duration, but it is not allowed to exceed 400 kW/m^2.

Step 6: Calculate the maximum view factor from a differential target (at specific grade level locations outside the fireball) to the fireball, using the simple equation for a spherical radiator [Howell, 1982].

$$F = \frac{R^2}{H^2}$$

where: F = view factor from differential area to the fireball, dimensionless
R = radius of the fireball, m
H = distance between target and the center of the fireball, m

R and H vary with time due to the growth and rise of the fireball. Therefore, the duration of the fireball is divided into time intervals and a view factor is calculated at the end of each interval.

Step 7: Compute the attenuated radiant heat flux at each target location, at the end of each time interval, by multiplying the appropriate view factor by the surface flux of the fireball and by the appropriate atmospheric transmittance. The transmittance of the atmosphere is a function of the absolute humidity and path length from the fireball to the target [Wayne, 1991]. For each target location, calculate the average attenuated heat flux over the duration of the fireball.

Step 8: Calculate the absorbed energy at each target location. For a given location, the energy absorbed during each time interval is computed by multiplying the length of the interval by the average attenuated radiant heat flux for that interval. The absorbed energies for all time intervals are then summed to determine the radiant energy absorbed over the duration of the fireball.

Step 9: Calculate the integrated dosage at each target location. This is computed in the same manner as absorbed energy is computed in Step 8, except that the average attenuated radiant heat flux for each time interval is taken to the 4/3rds power before it is multiplied by the time interval. This allows the dosage to be used in the probit equation for fatalities from thermal radiation [Eisenberg, Lynch, and Breeding, 1975].

$$Pr = -38.4785 + 2.56 \cdot \ln \left(q^{4/3} \cdot t \right)$$

where: Pr = probit
         q = radiant heat flux, W/m^2
         t = exposure time, s

Validation

Several of the equations used in the Fireball Model are empirical relationships based on data from small- to medium-scale experiments, which ensures reasonably good agreement between model predictions and experimental data for variables such as maximum fireball diameter. Comparisons of experimental data and model predictions for average incident heat flux, absorbed energy, or dosage are more meaningful and of greater interest. Unfortunately, very few reports on small- or medium-scale fireball experiments contain the level of detail required to make such comparisons, and no such data are available for large-scale experiments.

One of the most complete sources of test data for medium-scale fireball tests is a report by Johnson, Pritchard, and Wickens [1990]. It contains data on five BLEVE tests that involved butane and propane, in quantities up to 2,000 kg. Figure D-1 compares the predicted values of absorbed energy with experimental data from those five BLEVE tests.
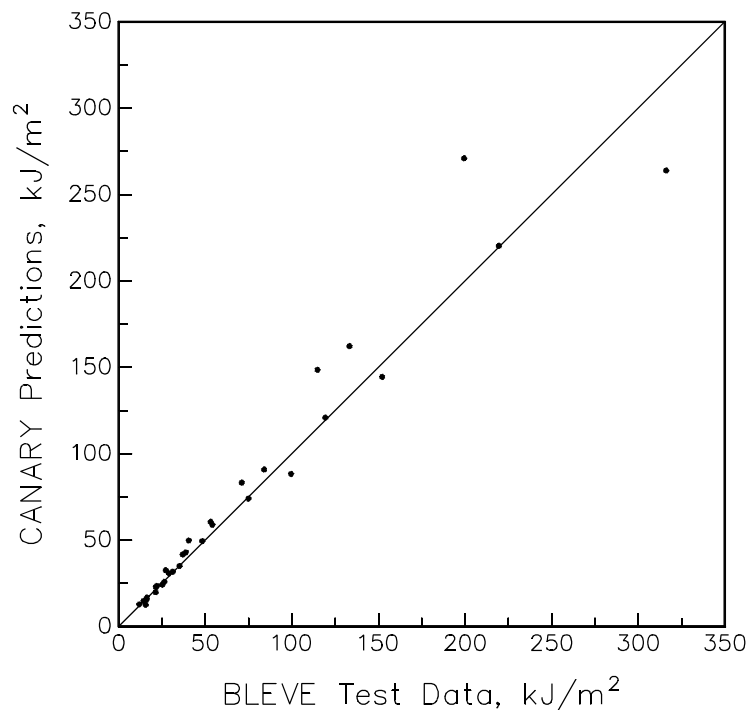

Figure D-1

References

Eisenberg, N. A., C. J. Lynch, and R. J. Breeding, *Vulnerability Model: A Simulation System for Assessing Damage Resulting from Marine Spills*. U.S. Coast Guard, Report CG-D-136-75, June, 1975.

Hasegawa, K., and K. Sato, "Study on the Fireball Following Steam Explosion of *n*-Pentane." *Proceedings of the Second International Symposium on Loss Prevention and Safety Promotion in the Process Industries*, Heidelberg, Germany, September, 1977: pp. 297-304.

Howell, John R., *A Catalog of Radiation Configuration Factors*. McGraw-Hill Book Company, 1982.

Johnson, D. M., M. J. Pritchard, and M. J. Wickens, *Large-Scale Catastrophic Releases of Flammable Liquids*. Commission of European Communities, Report EV4T.0014, 1990.

Martinsen, W. E., and J. D. Marx, "An Improved Model for the Prediction of Radiant Heat from Fireballs." Presented at the 1999 International Conference and Workshop on Modeling Consequences of Accidental Releases of Hazardous Materials, San Francisco, California, September 28 - October 1, 1999.

Roberts, A. F., "Thermal Radiation Hazards from Releases of LPG from Pressurized Storage." *Fire Safety Journal*, Vol. 4, 1981/82: pp. 197-212.

Shield, S. R., *Consequence Modeling for LPG Distribution in Hong Kong*. Thornton Research Centre, Safety and Environment Department, United Kingdom, TNRN 95.7001, December 13, 1994.

Wayne, F. D., "An Economical Formula for Calculating Atmospheric Infrared Transmissivities." *Journal of Loss Prevention in the Process Industries*, Vol. 4, January, 1991: pp. 86-92.

Fluid Release Model

Purpose

The purpose of the Fluid Release Model is to predict the rate of mass release from a breach of containment. Specifically, the model predicts the rate of flow and the physical state (liquid, two-phase, or gas) of the release of a fluid stream as it enters the atmosphere from a circular breach in a pipe or vessel wall. The model also computes the amount of vapor and aerosol produced and the rate at which liquid reaches the ground.

Required Data

(a)   Composition of the fluid
(b)   Temperature and pressure of the fluid just prior to the time of the breach
(c)   Normal flow rate of fluid into the vessel or in the pipe
(d)   Size of the pipe and/or vessel
(e)   Length of pipe
(f)   Area of the breach
(g)   Angle of release relative to horizontal
(h)   Elevation of release point above grade

Methodology

Step 1: Calculation of Initial Flow Conditions

The initial conditions (before the breach occurs) in the piping and/or vessel are determined from the input data, coupled with a calculation to determine the initial pressure profile in the piping. The pressure profile is computed by dividing the pipe into small incremental lengths and computing the flow conditions stepwise from the vessel to the breach point. As the flow conditions are computed, the time required for a sonic wave to traverse each section is also computed. The flow in any length increment can be all vapor, all liquid, or two-phase (this implies that the sonic velocity within each section may vary). As flow conditions are computed in each length increment, checks are made to determine if the fluid velocity has exceeded the sonic velocity or if the pressure in the flow increment has reached atmospheric. If either condition has been reached, an error code is generated and computations are stopped.

Step 2: Initial Unsteady State Flow Calculations

When a breach occurs in a system with piping, a disturbance in flow and pressure propagates from the breach point at the local sonic velocity of the fluid. During the time required for the disturbance to reach the upstream end of the piping, a period of highly unsteady flow occurs. The portion of the piping that has experienced the passage of the pressure disturbance is in accelerated flow, while the portion upstream of the disturbance is in the same flow regime as before the breach occurred.

To compute the flow rate from the breach during the initial unsteady flow period, a small time increment is selected and the distance that the pressure disturbance has moved in that time increment is computed using the sonic velocity profile found in the initial pressure profile calculation. The

disturbed length is subdivided into small increments for use in an iterative pressure balance calculation. A pressure balance is achieved when a breach pressure is found that balances the flow from the breach and the flow in the disturbed section of piping. Another time increment is added, and the iterative procedure continues. The unsteady period continues until the pressure disturbance reaches the upstream end of the pipe.

Step 3: Long-Term Unsteady State Flow Calculations

The long-term unsteady state flow calculations are characterized by flow in the piping system that is changing more slowly than during the initial unsteady state calculations. The length of accelerated flow in the piping is constant, set by the user input pipe length. The vessel contents are being depleted, resulting in a potential lowering of pressure in the vessel. As with the other flow calculations, the time is incremented and the vessel conditions are computed. The new vessel conditions serve as input for the pressure drop calculations in the pipe. When a breach pressure is computed that balances the breach flow with the flow in the piping, a solution for that time is achieved. The solution continues until the ending time or other ending conditions are reached.

The frictional losses in the piping system are computed using the equation:

$$h = \left(\frac{4 \cdot f \cdot L \cdot U_{ls}^2}{2 \cdot g_c \cdot D_e} \right) \tag{1}$$

where: h = head (pressure) loss, ft of fluid
$\quad\quad f$ = friction factor
$\quad\quad L$ = length of system, ft
$\quad\quad U$ = average flowing velocity, ft/sec
$\quad\quad g_c$ = gravitational constant, 32.2 $lb_m \cdot ft/(lb_f \cdot sec^2)$
$\quad\quad D_e$ = equivalent diameter of duct, ft

The friction factor is computed using the following equation:

$$\frac{1}{\sqrt{f}} = 1.74 - 2.0 \cdot \log_{10} \left[\frac{2 \cdot \varepsilon}{D_e} + \frac{18.7}{Re \cdot \sqrt{f}} \right] \tag{2}$$

where: ε = pipe roughness, ft
$\quad\quad Re$ = Reynolds number, $D_e \cdot U \cdot \rho / \mu$, dimensionless
$\quad\quad \rho$ = fluid density, lb/ft^3
$\quad\quad \mu$ = fluid viscosity, $lb/(ft \cdot sec)$

Equations (1) and (2) are used for liquid, vapor, and two-phase flow regimes. Since the piping is subdivided into small lengths, changes in velocity and physical properties across each segment are assumed to be negligible. At each step in the calculation, a check is made to determine if the fluid velocity has reached or exceeded the computed critical (sonic) velocity for the fluid. If the critical velocity has been exceeded, the velocity is constrained to the critical velocity and the maximum mass flow rate in the piping has been set.

If the fluid in the piping is in two-phase flow, the Lockhart and Martinelli [1949] modification to Equation (1) is used. The Lockhart and Martinelli equation for head loss is shown below:

$$h_{TP} = \Phi^2 \cdot \left(\frac{4 \cdot f \cdot L \cdot U_{ls}^2}{2 \cdot g_c \cdot D_e} \right)$$

(3)

where: h_{TP} = head loss for two-phase flow, ft of fluid

   Φ = empirical parameter correlating single- and two-phase flow, dimensionless

   U_{ls} = superficial liquid velocity (velocity of liquid if liquid filled the pipe), ft/sec

This equation is valid over short distances where the flowing velocity does not change appreciably.

Validation

Validation of fluid flow models is difficult since little data are available for comparison. Fletcher [1983] presented a set of data for flashing CFC-11 flowing through orifices and piping. Figures E-1 through E-4 compare calculations made using the Fluid Release Model with the data presented by Fletcher. Figure E-1 compares fluid fluxes for orifice type releases. These releases had length-to-diameter (L/D) ratios less than 0.88. Figure E-2 compares computed and experimental release fluxes for an L/D ratio of 120 at several levels of storage pressure. Figure E-3 compares similar releases for an L/D of 37.5. Figure E-4 shows predicted and experimental release fluxes at a given pressure for L/D ratios from 1 to 200.

Figures E-5 and E-6 compare computed and experimental gas discharge rates for the complete breach of two pipes. One pipe had an internal diameter of 6.2 inches (0.157 m); the other had a diameter of 12 inches (0.305 m). These pipes were initially pressurized to 1,000 psia with air and then explosively ruptured. The experimental values were reported in a research paper for Alberta Environment, authored by Wilson [1981].

Aerosols and Liquid Droplet Evaporation

Liquids stored at temperatures above their atmospheric pressure boiling point (superheated liquids) will give off vapor when released from storage. If the temperature of storage is sufficiently above the normal boiling point, the energy of the released vapor will break the liquid stream into small droplets. If these droplets are small enough, they will not settle, but remain in the vapor stream as aerosol droplets. The presence of aerosol droplets in the vapor stream changes its apparent density and provides an additional source of vapor. Droplets large enough to fall to the ground will lose mass due to evaporation during their fall.

The prediction of aerosol formation and amount of aerosol formed is based on the theoretical work performed for the Center for Chemical Process Safety (CCPS) by CREARE. CREARE's work has been extended and corrected by Quest. The extension to the model computes the non-aerosol drop evaporation. In Figure E-7, the four experimental data sets available for comparison (chlorine (Cl_2), methylamine (MMA), CFC-11, and cyclohexane) are compared to the values computed by the CANARY Aerosol Model.
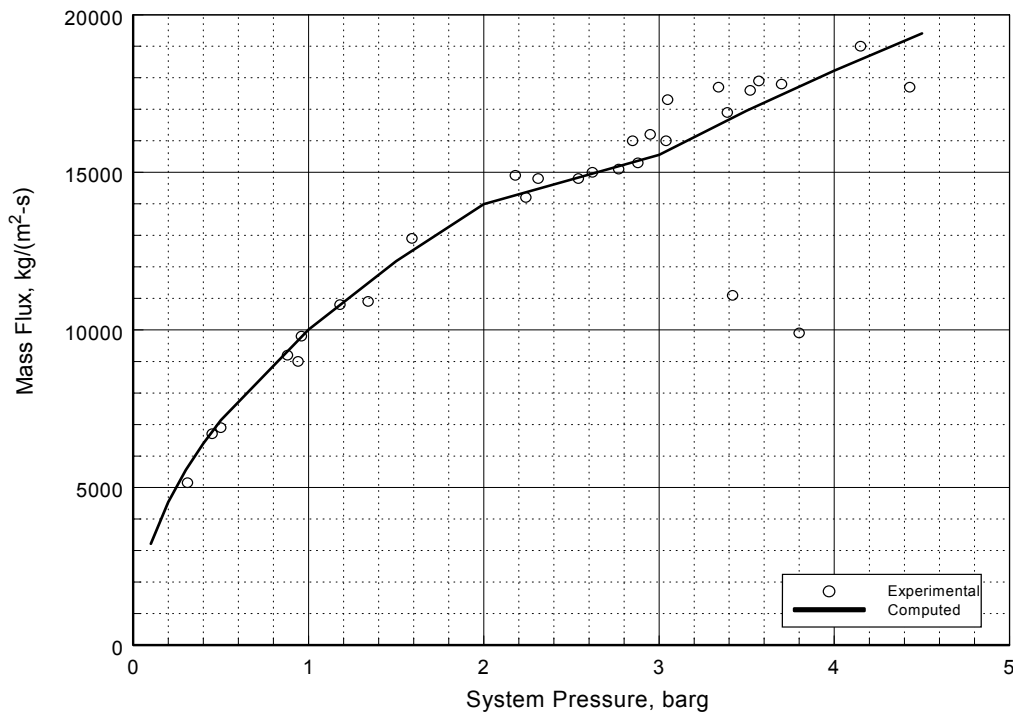
Figure E-1
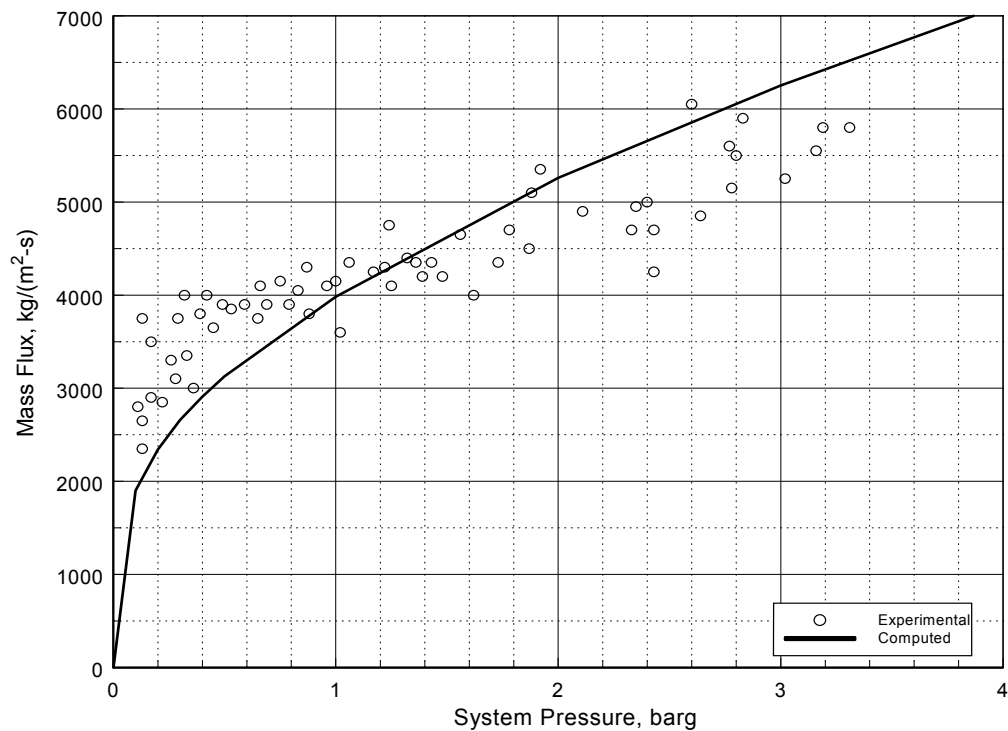**Comparison of CFC-11 Orifice Releases as a Function of System Pressure**

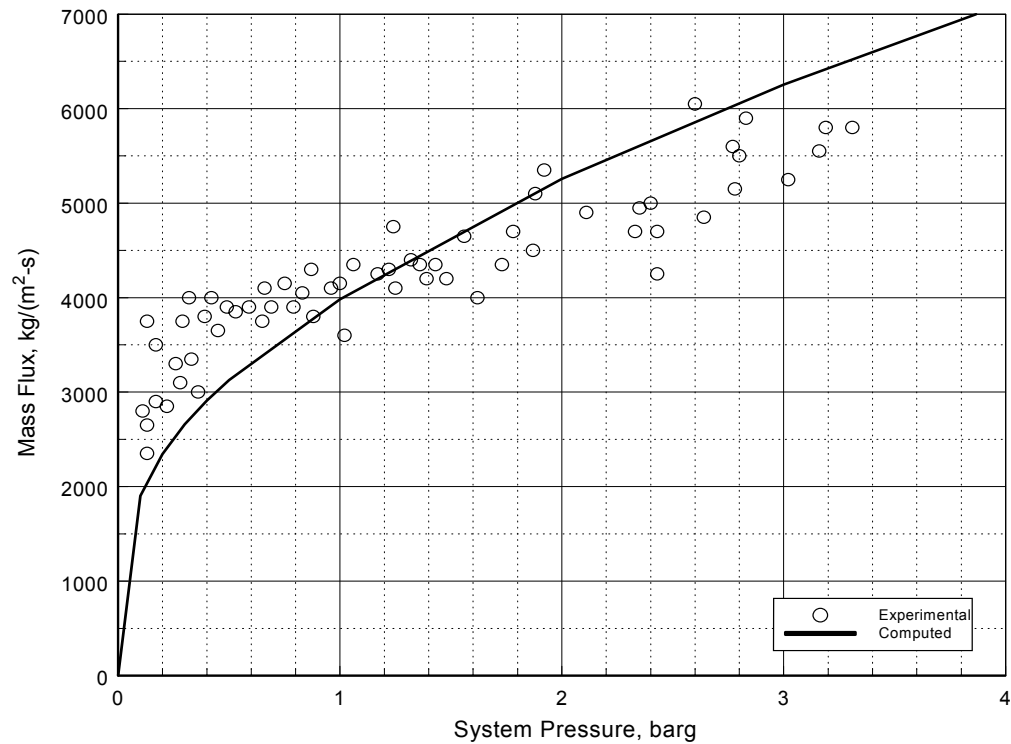**Figure E-2**
CFC-11 Release Rate Comparison with L/D of 120

Figure E-3
CFC-11 Release Rate Comparison with L/D of 37.5
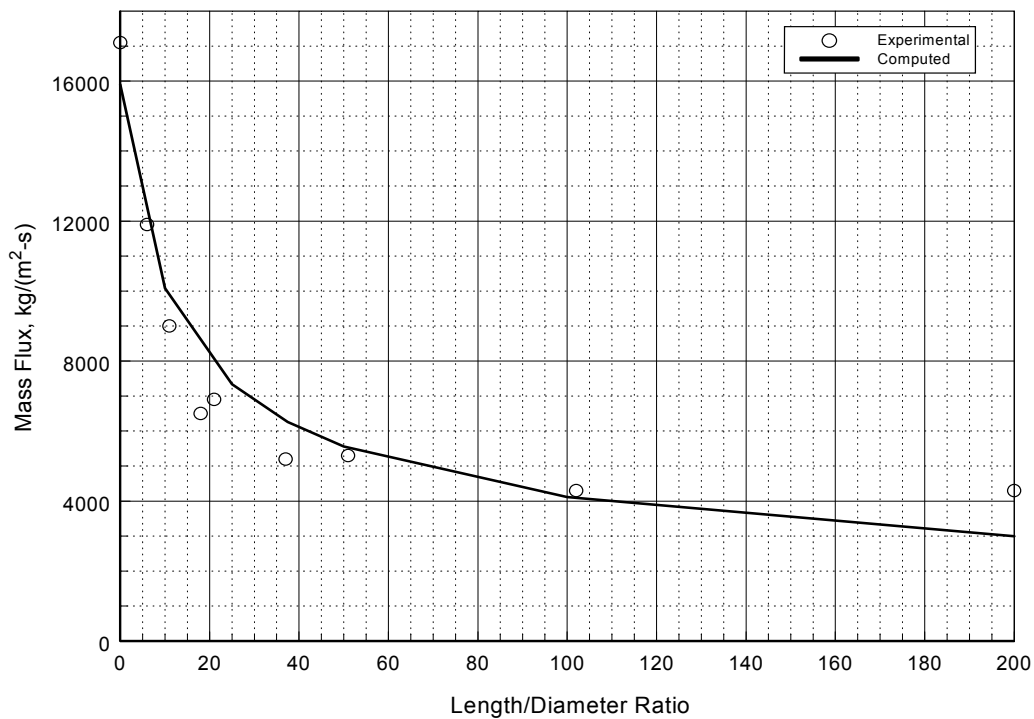

Figure E-4
CFC-11 Release Rate Comparison at Varying L/D Ratios
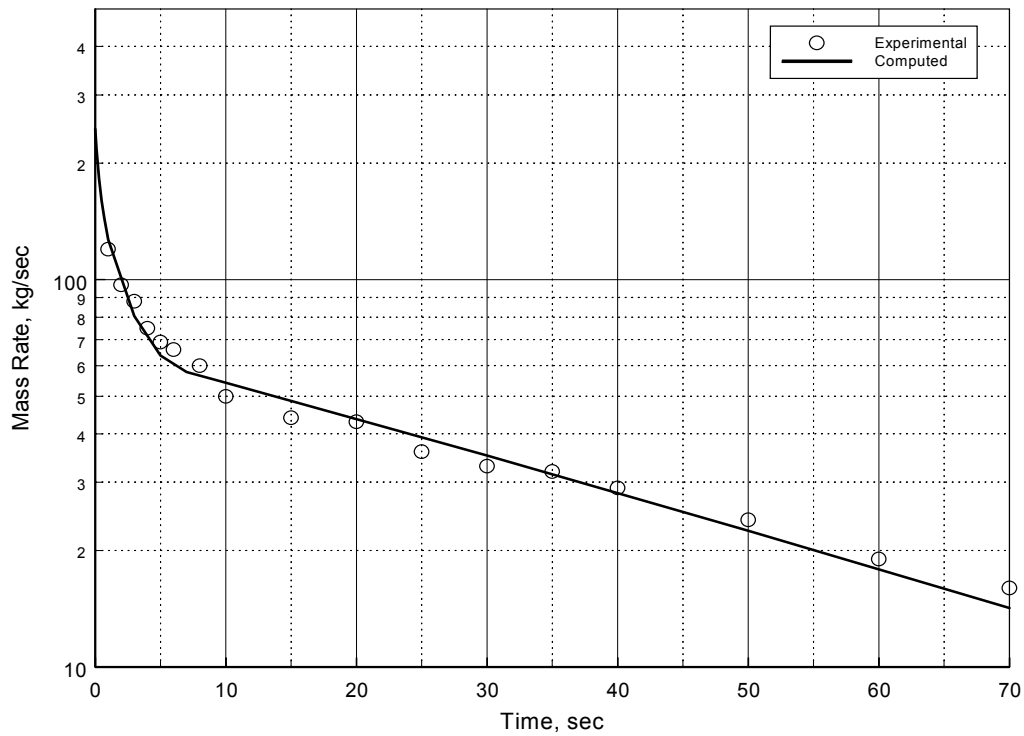
Figure E-5
Air Discharge Rates for 0.157 m Diameter Piping

Figure E-6
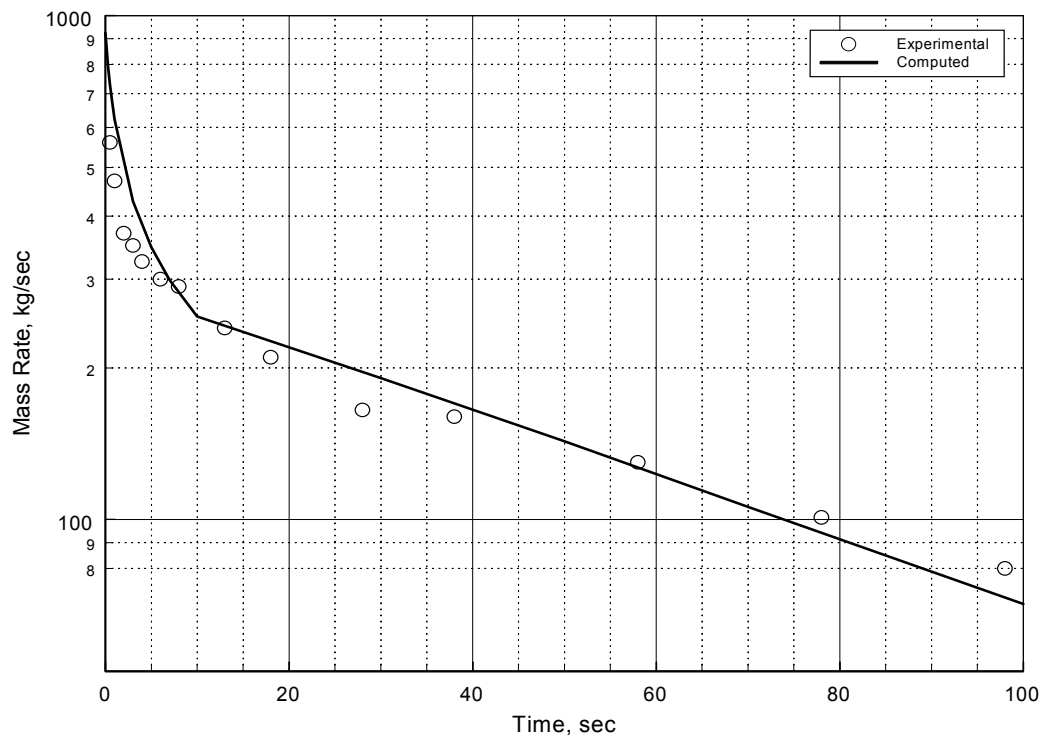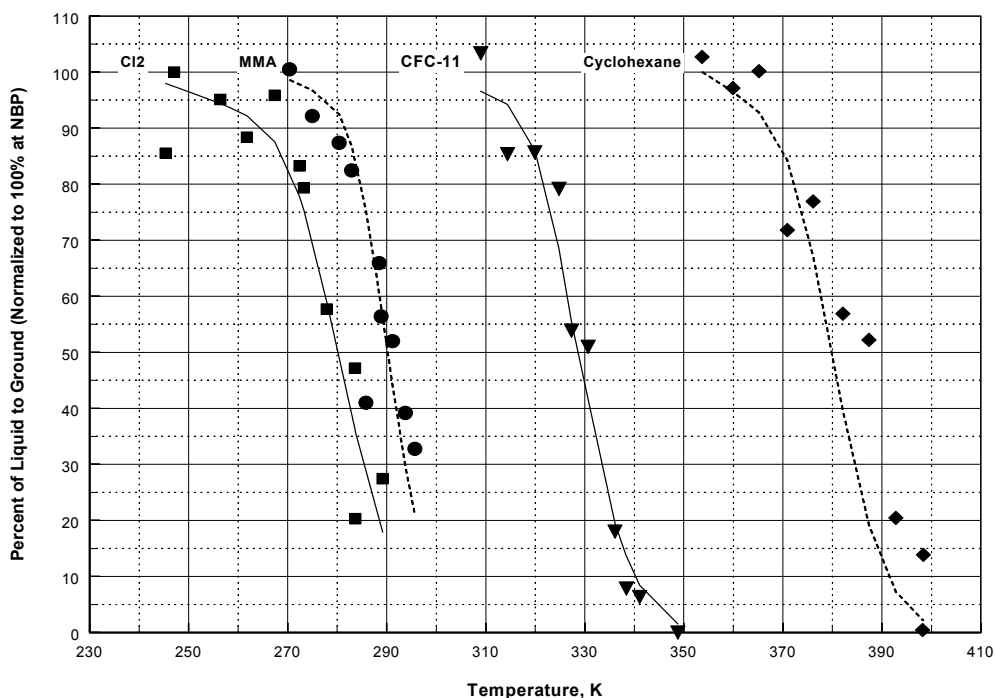**Air Discharge Rates for 0.305 m Diameter Piping**

Figure E-7
Aerosol Formation as a Function of Storage Temperature

References

Fletcher, B., "Flashing Flow Through Orifices and Pipes." Paper presented at the AIChE Loss Prevention Symposium, Denver, Colorado, 1983.

Lockhart, R. W., and R. C. Martinelli, "Proposed Correlation of Data for Isothermal Two-Phase, Two-Component Flow in Pipes." Chemical Engineering Progress, Vol. 45, 1949: p. 39.

Wilson, D. J., "Expansion and Plume Rise of Gas Jets from High Pressure Pipeline Ruptures." Research Paper, Pollution Control Division, Alberta Environment, April, 1981.

Momentum Jet Dispersion Model

Purpose

The purpose of this model is to predict the dispersion of a jet release into ambient air. It is used to predict the downwind travel of a flammable or toxic gas or aerosol momentum jet release.

Required Data

(a)	Composition and properties of the released material
(b)	Temperature of released material
(c)	Release rate of material
(d)	Vertical release angle relative to wind direction
(e)	Height of release
(f)	Release area
(g)	Ambient wind speed
(h)	Ambient Pasquill-Gifford stability class
(i)	Ambient temperature
(j)	Relative humidity
(k)	Surface roughness scale

Methodology

Step 1: An assumption is made that flow perpendicular to the main flow in the plume is negligible, that the velocity and concentration profiles in the jet are similar at all sections of the jet, that molecular transport in the jet is negligible, and that longitudinal turbulent transport is negligible when compared to longitudinal convective transport. The coordinate system is then defined in s and r, where s is the path length of the plume and r is the radial distance from the plume centerline. The angle between the plume axis and horizontal is referred to as θ. Relationships between the downwind coordinate, x, vertical coordinate, y, and plume axis are given simply by:

$$\frac{dx}{ds} = \cos(\theta) \tag{1}$$

and

$$\frac{dy}{ds} = \sin(\theta) \tag{2}$$

Step 2: Velocity, concentration, and density profiles are assumed to be cylindrically symmetric about the plume axis and are assumed to be Gaussian in shape. The three profiles are taken as:

$$u(s,r,\theta) = U_a \cdot \cos(\theta) + u^*(s) \cdot e^{\frac{-r^2}{b^2(s)}} \tag{3}$$

where: u = plume velocity, m/s
U_a = ambient wind speed, m/s
u^* = plume velocity relative to the wind in the downwind direction at the plume axis, m/s
$b(s)$ = characteristic width of the plume at distance s from the release, m

$$\rho(s, r, \theta) = \rho_a + \rho^*(s) \cdot e^{\frac{-r^2}{\lambda^2 \cdot b^2(s)}} \tag{4}$$

where: ρ = plume density, kg/m^3
ρ_a = density of ambient air, kg/m^3
$\rho^*(s)$ = density difference between plume axis and ambient air, kg/m^3
λ^2 = turbulent Schmidt number, 1.35

$$c(s,r,\theta) = c^*(s) \cdot e^{\frac{-r^2}{\lambda^2 \cdot b^2(s)}} \tag{5}$$

where: c = pollutant concentration in the plume, kg/m^3
$c^*(s)$ = pollutant concentration at plume centerline, kg/m^3

Step 3: The equation for air entrainment into the plume and the conservation equations can then be solved. The equation for air entrainment is:

$$\frac{d}{ds}\left(\int_0^{b\sqrt{2}} \rho \cdot u \cdot 2 \cdot \pi \cdot dr\right) \tag{6}$$

$$= 2 \cdot \pi \cdot b \cdot \rho_a \cdot \left\{\alpha_1 \cdot |u^*(s)| + \alpha_2 \cdot U_a \cdot |\sin(\theta)|\cos(\theta) + \alpha_3 \cdot u'\right\}$$

where: α_1 = entrainment coefficient for a free jet, 0.057
α_2 = entrainment coefficient for a line thermal, 0.5
α_3 = entrainment coefficient due to turbulence, 1.0
u' = turbulent entrainment velocity (root mean square of the wind velocity fluctuation is used for this number), m/s

Step 4: The equations of conservation of mass, momentum, and energy are given as:

$$\frac{d}{ds}\left(\int_0^{b\sqrt{2}} c \cdot u \cdot 2 \cdot \pi \cdot dr\right) = 0 \tag{7}$$

$$\frac{d}{ds}\left(\int_0^{b\sqrt{2}} \left(\rho \cdot u^2 \cdot \cos(\theta) \cdot 2 \cdot \pi \cdot dr\right)\right) \tag{8}$$

$$= 2 \cdot \pi \cdot b \cdot \rho_a \cdot \left\{\alpha_1 \cdot |u^*(s)| + \alpha_2 \cdot U_a \cdot |\sin(\theta)| \cdot \cos(\theta) + \alpha_3 \cdot u'\right\}$$

$$+ C_d \cdot \pi \cdot b \cdot \rho_a \cdot U_a^2 |\sin(\theta)|$$

$$\frac{d}{ds}\left(\int_0^{b\sqrt{2}} \rho \cdot u^2 \cdot \cos(\theta) \cdot 2 \cdot \pi \cdot dr\right) \tag{9}$$

$$= \int_0^{b\sqrt{2}} g \cdot (\rho_a - \rho)\,\pi \cdot r \cdot dr \pm C_d \cdot \pi \cdot b \cdot \rho_a \cdot U_a^2 \cdot \sin(\theta) \cdot \cos(\theta)$$

$$\frac{d}{ds}\left(\int_0^{b\sqrt{2}} \rho \cdot u \left(\frac{1}{\rho} - \frac{1}{\rho_{a0}}\right) \cdot 2 \cdot \pi \cdot r \cdot dr\right) \tag{10}$$

$$= \rho_a \cdot 2 \cdot \pi \cdot b \left(\frac{1}{\rho_a} - \frac{1}{\rho_{a0}}\right) \cdot \left\{\alpha_1 \cdot |u^*(s)| + \alpha_2 \cdot U_a\,\sin(\theta)| \cdot \cos(\theta) + \alpha_3 \cdot \acute{u}\right\}$$

The subscript 0 refers to conditions at the point of release. These equations are integrated along the path of the plume to yield the concentration profiles as a function of elevation and distance downwind of the release.

Step 5: After the steady-state equations are solved, an along-wind dispersion correction is applied to account for short-duration releases. This is accomplished using the method outlined by Palazzi, et al. [1982].

Step 6: If the plume reaches the ground, it is coupled to the Heavy Gas Dispersion Model (described in Section G) and the dispersion calculations continue.

Validation

The Momentum Jet Dispersion Model used in CANARY was validated by comparing results obtained from the model with experimental data from field tests. Data used for this comparison and the conditions used in the model were taken from an American Petroleum Institute (API) study [Hanna, Strimaitis, and Chang, 1991]. For this model, comparisons were made with the Desert Tortoise, Goldfish, and Prairie Grass series of dispersion tests. Results of these comparisons are shown in Figure F-1.

References

Astleford, W. J., T. B. Morrow, and J. C. Buckingham, *Hazardous Chemical Vapor Handbook for Marine Tank Vessels* (Final Report – Phase II). U.S. Coast Guard Report No. CG-D-12-83, April, 1983.

Hanna, S. R., D. G. Strimaitis, and J. C. Chang, *Hazard Response Modeling Uncertainty (A Quantitative Method), Evaluation of Commonly Used Hazardous Gas Dispersion Models*, Volume II. Study co-sponsored by the Air Force Engineering and Services Center, Tyndall Air Force Base, Florida, and the American Petroleum Institute; performed by Sigma Research Corporation, Westford, Massachusetts, September, 1991.

Havens, J., and T. Spicer, *LNG Vapor Dispersion Prediction with the DEGADIS Dense Gas Dispersion Model*. Gas Research Institute Contract No. 5086-252-1287 with the University of Arkansas, September, 1990: pp. 37-48.

Ooms, G., "A New Method for the Calculation of the Plume Path of Gases Emitted by a Stack." *Atmospheric Environment*, Vol. 6, 1972: pp. 889-909.
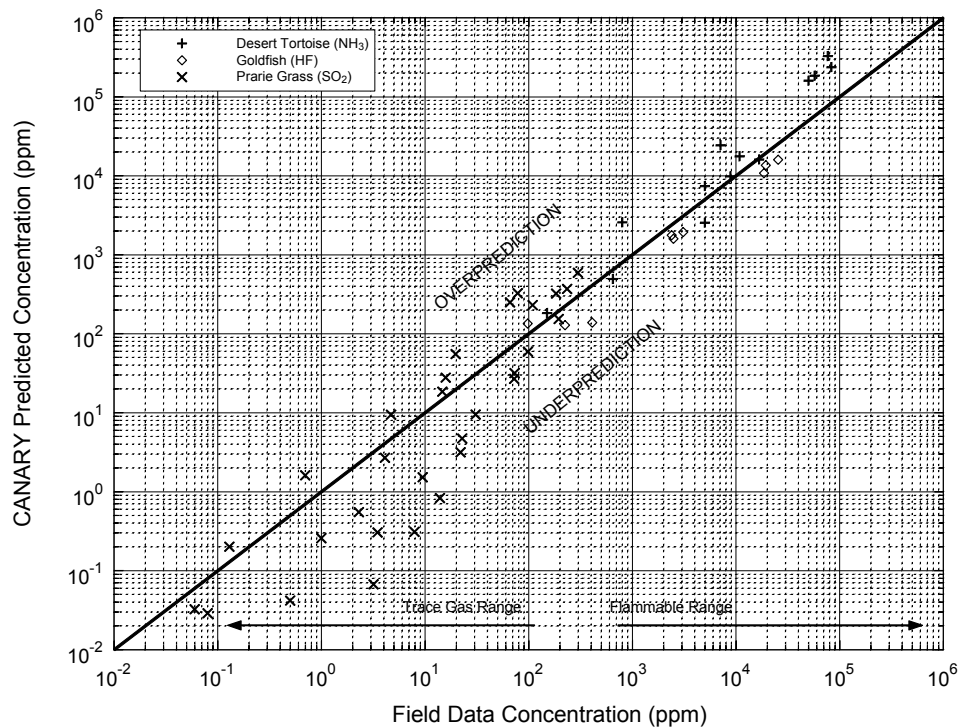
Figure F-1

Ooms, G., A. P. Mahieu, and F. Zelis, "The Plume Path of Vent Gases Heavier than Air." *First International Symposium on Loss Prevention and Safety Promotion in the Process Industries*, C. H. Buschman, Editor, Elsevier Press, 1974.

Palazzi, E., M. De Faveri, G. Fumarola, and G. Ferraiolo, "Diffusion from a Steady Source of Short Duration." *Atmospheric Environment*, Vol. 16, No. 12, 1982: pp. 2785-2790.

Heavy Gas Dispersion Model

Purpose

The purpose of this model is to predict the dispersion and gravity flow of a heavy gas released into the air from liquid pools or instantaneous gas releases. It is used to predict the downwind travel of a flammable or toxic vapor cloud.

Required Data

(a)   Composition and properties of the released material
(b)   Temperature of released material
(c)   Vapor generation rate
(d)   Vapor source area
(e)   Vapor source duration
(f)   Ambient wind speed
(g)   Ambient Pasquill-Gifford atmospheric stability class
(h)   Ambient temperature
(i)   Relative humidity
(j)   Surface roughness scale

Methodology

Step 1: For a steady-state plume, released from a stationary source, the Heavy Gas Dispersion Model solves the following equations:

$$\frac{d}{dx}\left(\rho \cdot U \cdot B \cdot h \cdot m\right) = \rho_s \cdot W_s \cdot B_s \tag{1}$$

$$\frac{d}{dx}\left(\rho \cdot U \cdot B \cdot h\right) = \rho_a \cdot \left(V_e \cdot h + W_e \cdot B\right) + \rho_s \cdot W_s \cdot B_s \tag{2}$$

$$\frac{d}{dx}\left(\rho \cdot U \cdot B \cdot h \cdot C_p \cdot T\right) = \rho_a \cdot \left(V_e \cdot h + W_e \cdot B\right) \cdot C_{pa} \cdot T_a + \rho_s \cdot W_s \cdot B_s \cdot C_{ps} \cdot T_s + f_t \tag{3}$$

$$\frac{d}{dx}\left(\rho \cdot U \cdot B \cdot h \cdot U\right)$$
$$= -0.5 \cdot \alpha_g \cdot g \cdot \frac{d}{dx}\left[\left(\rho - \rho_a\right) \cdot B \cdot h^2\right] + \rho_a \cdot \left(V_e \cdot h + W_e \cdot B\right) \cdot U_a + f_u \tag{4}$$

$$\frac{d}{dx}\left(\rho \cdot U \cdot B \cdot h \cdot V_g\right) = g \cdot \left(\rho - \rho_a\right) \cdot h^2 + f_{vg} \tag{5}$$

$$U \cdot \frac{dZ_c}{dx} = -V_g \cdot \frac{Z_c}{B} \tag{6}$$

$$U \cdot \frac{dB}{dx} = \frac{\rho_a}{\rho} \cdot V_e + V_g \tag{7}$$

$$\rho \cdot T = \frac{\rho_a \cdot T_a \cdot M_s}{\left[M_s + \left(M_a - M_s \right) \cdot m \right]} \tag{8}$$

where: x = downwind distance, m
ρ = density, kg/m³
U = velocity in the direction of the wind, m/s
B = cloud width parameter, m
h = cloud height parameter, m
m = mass fraction of source gas
T = temperature, K
C_p = specific heat, J/(kg · K)
f_t = ground heat flux, J/(m · s)
f_u = downwind friction term, kg/s²
f_v = crosswind friction term, kg/s²
V_e = horizontal entrainment rate, m/s
V_g = horizontal crosswind gravity flow velocity, m/s
W_e = vertical entrainment rate, m/s
W_s = vertical source gas injection velocity, m/s
M = molecular weight, kg/kmole
s = refers to source properties
a = refers to ambient properties

The first six equations are crosswind-averaged conservation equations. Equation (7) is the width equation, and Equation (8) is the equation of state.

Step 2: All of the gas cloud properties are crosswind averaged. The three-dimensional concentration distribution is calculated from the average mass concentration by assuming the following concentration profile:

$$C \left(x, y, z \right) = C \left(x \right) \cdot C_1 \left(y \right) \cdot C_2 \left(z \right) \tag{9}$$

$$C \left(x \right) = \frac{M_a \cdot m \left(x \right)}{M_s + \left(M_a - M_s \right) \cdot m \left(x \right)} \tag{10}$$

$$C_1 \left(y \right) = \frac{1}{4 \cdot b} \cdot \left\{ erf \left(\frac{y+b}{2 \cdot \beta} \right) - erf \left(\frac{y-b}{2 \cdot \beta} \right) \right\} \tag{11}$$

$$B^2 = b^2 + 3 \cdot \beta^2 \tag{12}$$

$$C_2(z) = \left(\frac{6}{\pi}\right)^{1/2} \cdot \frac{1}{h} \cdot \exp\left(\frac{-3 \cdot z^2}{2 \cdot h^2}\right) \tag{13}$$

where: $C(x, y, z)$ = concentration in plume at $x, y, z,$ kg/m³
   y = crosswind coordinate, m
   z = vertical coordinate, m
   b, B, β = half-width parameters, m

Step 3: As there are now two parameters used to define $C_1(y)$, the following equation is needed to calculate b:

$$U \cdot \left(\frac{db}{dx}\right) = V_g \cdot \frac{b}{B} \tag{14}$$

Step 4: The vertical entrainment rate is defined to be:

$$W_e = \frac{\sqrt{3} \cdot a \cdot k \cdot U_* \cdot \delta\left(\frac{h}{H}\right)}{\Phi_h\left(\frac{h}{L}\right)} \tag{15}$$

where: a = constant, 1.5
   k = constant, 0.41
   U_* = friction velocity, m/s
   L = Monin-Obukhov length derived from the atmospheric stability class

Step 5: The profile function δ is used to account for the height of the mixing layer, H, and to restrict the growth of the cloud height to that of the mixing layer. H is a function of stability class and is defined as:

$$\delta\left(\frac{h}{H}\right) = 1 - \frac{h}{H} \tag{16}$$

The Monin-Obukhov function, Φ_h, is defined by:

$$\Phi_h\left(\frac{h}{L}\right) = \begin{cases} 1 + 5 \cdot \dfrac{h}{L} & L \geq 0 \text{ (stable)} \\[2ex] \left[1 - 16 \cdot \dfrac{h}{L}\right]^{-1/2} & L < 0 \text{ (unstable)} \end{cases} \tag{17}$$

Step 6: After the steady-state equations are solved, an along-wind dispersion correction is applied to account for short-duration releases. This is accomplished using the method outlined by Palazzi, et al. [1982].

Validation

The Heavy Gas Dispersion Model used in CANARY was validated by comparing results obtained from the model with experimental data from field tests. Data used for this comparison and the conditions used in the model were taken from an American Petroleum Institute (API) study [Hanna, Strimaitis, and Chang, 1991]. For this model, comparisons were made with the Burro, Maplin Sands, and Coyote series of dispersion tests. Results of these comparisons are shown in Figure G-1.
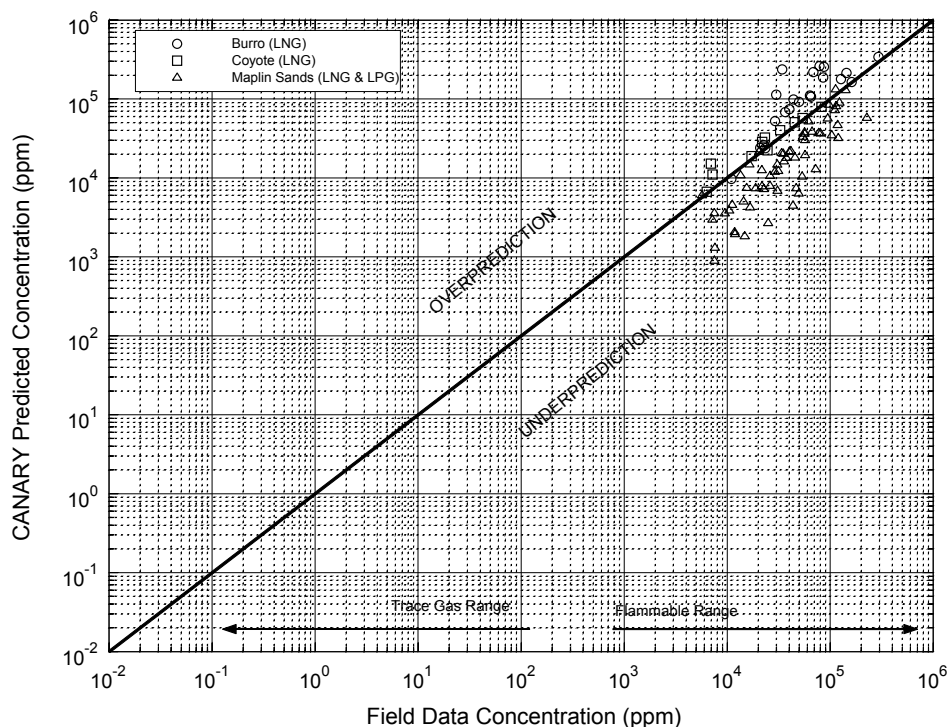

Figure G-1

References

Ermak, D. L., and S. T. Chan, *A Study of Heavy Gas Effects on the Atmospheric Dispersion of Dense Gases*. UCRL-92494, Lawrence Livermore National Laboratory, Livermore, California. Presented at the 15th NATO/CCMS International Technical Meeting on Air Pollution Modeling and Its Applications, St. Louis, Missouri, April 15-19, 1985.

Ermak, D. L., S. T. Chan, D. L. Morgan, Jr., and L. K. Morris, "A Comparison of Dense Gas Dispersion Model Simulations with Burro Series LNG Spill Test Results." *Journal of Hazardous Materials*, Vol. 6, 1982: pp. 129-160.

Ermak, D. L., and S. T. Chan, *Recent Developments on the FEM3 and SLAB Atmospheric Dispersion Models*. UCRL-94071, Lawrence Livermore National Laboratory, Livermore, California. Presented at the IMA Conference on Stably Stratified Flows and Dense Gas Dispersion, Chester, England, April 9-10, 1986.

Hanna, S. R., D. G. Strimaitis, and J. C. Chang, *Hazard Response Modeling Uncertainty (A Quantitative Method), Evaluation of Commonly-Used Hazardous Gas Dispersion Models*, Volume II. Study cosponsored by the Air Force Engineering and Services Center, Tyndall Air Force Base, Florida, and the

American Petroleum Institute; performed by Sigma Research Corporation, Westford, Massachusetts, September, 1991.

Morgan, D. L., L. K. Morris, S. T. Chan, D. L. Ermak, T. G. McRae, R. T. Cederwall, R. P. Kooperman, H. C. Goldwire, Jr., J. W. McClure, and W. J. Hogan, *Phenomenology and Modeling of Liquefied Natural Gas Vapor Dispersion*. UCRL-53581, Lawrence Livermore National Laboratory, Livermore, California, 1982.

Morgan, D. L., Jr., L. K. Morris, and D. L. Ermak, *SLAB: A Time-Dependent Computer Model for the Dispersion of Heavy Gases Released in the Atmosphere*. UCRL-53383, Lawrence Livermore National Laboratory, Livermore, California, 1983.

Palazzi, E., M. De Faveri, G. Fumarola, and G. Ferraiolo, "Diffusion from a Steady Source of Short Duration." *Atmospheric Environment*, Vol. 16, No. 12, 1982: pp. 2785-2790.

Vapor Cloud Explosion Model

Purpose

The purpose of this model is to predict the overpressure field that would be produced by the explosion of a partially confined and/or obstructed fuel-air cloud, based on the Baker-Strehlow methodology. Specifically, the model predicts the magnitude of the peak side-on overpressure and specific impulse as a function of distance from the source of the explosion.

Required Data

(a) Composition of the fuel (flammable fluid) involved in the explosion
(b) Total mass of fuel in the flammable cloud at the time of ignition or the volume of the partially-confined/obstructed area
(c) Fuel reactivity (high, medium, or low)
(d) Obstacle density (high, medium, or low)
(e) Flame expansion (1-D, 2-D, 2½-D, or 3-D)
(f) Reflection factor

Methodology

Step 1: The combustion energy of the cloud is estimated by multiplying its mass by the heat of combustion. If the volume of the flammable cloud is input, the mass is estimated by assuming that a stoichiometric mixture of gas and air exists within that volume.

Step 2: The combustion energy is multiplied by the reflection factor to account for blast reflection from the ground or surrounding objects.

Step 3: Flame speed is determined from the fuel reactivity, obstacle density, and flame expansion parameters, as presented in Baker, et al. [1994, 1998].

Fuel reactivity and obstacle density each have low, medium, and high choices. The flame expansion parameter allows choices of 1-D, 2-D, 2.5-D, and 3-D. The choices for these three parameters create a matrix of 36 possibilities, thus allowing locations that have differing levels of congestion or confinement to produce different overpressures. Each matrix possibility corresponds to a flame speed, and thus a peak (source) overpressure. The meanings of the three parameters and their options are:

Fuel Reactivity (High, Medium, or Low). The fuels considered to have high reactivity are acetylene, ethylene oxide, propylene oxide, and hydrogen. Low reactivity fuels are (pure) methane and carbon monoxide. All other fuels are medium reactivity. If fuels from different reactivity categories are mixed, the model recommends using the higher category unless the amount of higher reactivity fuel is less than 2% of the mixture.

Obstacle Density (High, Medium, or Low). High obstacle density is encountered when objects in the flame's path are closely spaced. This is defined as multiple layers of obstruction resulting in at least a 40% blockage ratio (i.e., 40% of the volume is occupied by

obstacles). Low density areas are defined as having a blockage ratio of less than 10%. All other blockage ratios fall into the medium category.

Flame Expansion (1-D, 2-D, 2.5-D, or 3-D). The expansion of the flame front must be characterized with one of these four descriptors. 1-D expansion is likened to an explosion in a pipe or hallway. 2-D expansion can be described as what occurs between flat, parallel surfaces. An unconfined (hemispherical expansion) case is described as 3-D. The additional descriptor of 2.5-D is used for situations that begin as 2-D and quickly transition to 3-D.

Step 4: Based on the calculated flame speed, appropriate blast curves are selected from the figures in Baker, et al., 1994. For flame speeds not shown on the graph, appropriate curves are prepared by interpolation between existing curves.

Step 5: The Sachs scaled distance, $\overline{R}$, is calculated for several distances using the equation:

$$\overline{R} \;=\; \frac{R}{\left(\dfrac{E}{P_0}\right)^{1/3}}$$

where: R = distance from the center of the explosion
E = total energy calculated in step 2, above
P_0 = atmospheric pressure

Step 6: The peak side-on overpressure and specific impulse at each scaled distance are determined from the blast curves in Baker, et al., 1994.

References

Baker, Q. A., M. J. Tang, E. Scheier, and G. J. Silva, "Vapor Cloud Explosion Analysis." *28th Loss Prevention Symposium, AIChE,* 1994.

Baker, Q. A., C. M. Doolittle, G. A. Fitzgerald, and M. J. Tang, "Recent Developments in the Baker-Strehlow VCE Analysis Methodology." *Process Safety Progress*, 1998: p. 297.